2026

COP
Circular Ocean-bound Plastic

# Chemical Recycling Options for Ocean-bound Plastic

Report

August 2026

Report on chemical and solvent-based recycling options for river-collected ocean-bound plastic

**Publisher**
Interreg South Baltic project
Circular Ocean-bound Plastic

**www.circularoceanplastic.eu**


**Authors**
Dr Eng. Patrycja Jutrzenka Trzebiatowska, MSc Kacper Pobłocki

**Contributors**
Dr Eng. Emilia Gontarek-Castro, Dr Eng. Onur Cavdar

**Partners in the COP project and contributors**
Clean - The Danish Water and Environmental Cluster (DK) - leadpartner
Ocean Plastic Forum (DK)
Danish Materials Network (DK)
Sustainable Business Hub (SE)
Leibniz Institute for Baltic Sea Research (DE)
University of Rostock (DE)
University of Gdansk (PL)
Gdansk Water Foundation (PL)
Gdansk Sport Center (PL)

**Layout**
Martin Pham, Clean - The Danish Water and Environmental Cluster

**ISBN** 978-87-975259-3-7 (digital)



**For more information**
To receive information about the project and other related publications, please visit www.circularoceanplastic.eu




# Contents


Summary 4

1. Introduction 7

    1.1 Project Context and Scope 7

    1.2 Challenges of Riverine Plastic 7

    1.3 Background on chemical Recycling of Ocean-Bound Plastic 8

2. Materials selected for solvent-based and chemical recycling:

    OBP fractions from Aarhus and Gdańsk 13

3. Solvent-based and chemical recycling options for OBP 17

    3.1 Green solvent-based recycling of polyolefins 17

    3.2 Glycolysis of PET 27

    3.3 Methanolysis of PC 35

    3.4 Pyrolysis of polyolefins (PE, PP) and PS 41

    3.5. Up-scale pyrolysis trials performed by Plast Center Danmark 52

    3.6 Comparison of laboratory- and up-scale pyrolysis experiments 54

4. Conclusion 58

5. Recommendations 61

6. Limitations of the study 64

7. References 67

# Summary

This report presents the evaluation of chemical and solvent-based recycling pathways for ocean-bound plastic (OBP) collected from the Motława River (Gdańsk, Poland) and the Aarhus River (Aarhus, Denmark) within the Interreg South Baltic project Circular Ocean-bound Plastic (COP). Based on previous project activities involving polymer identification, material characterisation, cleaning and mechanical recycling assessment, this deliverable investigates complementary recycling technologies capable of recovering value from collected OBP fractions.

The study addresses the main challenge associated with river-collected plastic, namely its heterogeneous composition, contamination, environmental ageing and variable material quality, which limit the direct application of conventional mechanical recycling. The objective was to identify technically feasible, polymer-specific recycling pathways and to assess their potential for recovering polymers, monomeric products or hydrocarbon-based feedstocks from selected OBP fractions.

The polymer composition analysis performed within the COP project demonstrated that collected OBP streams are dominated by common consumer polymers, particularly polyolefins (polyethylene - PE and polypropylene - PP) and poly(ethylene terephthalate) - PET. In Gdańsk, PE, PET and PP accounted for most identified plastic items, while in Aarhus, PP and PE represented the dominant fractions with additional contributions from PET and polycarbonate - PC. The suitability of individual fractions for recycling was governed not only by polymer identity but also by contamination level, environmental ageing, and product complexity, since no single recycling technology can effectively process the entire OBP stream.

Complementary to mechanical recycling pathways, additional approaches such as solvent-based recycling, solvolysis and pyrolysis were investigated. Solvent-based recycling (dissolution) was evaluated for relatively homogeneous polyolefin fractions to recover purified polymers through selective dissolution and precipitation with selected green solvents. Two common solvolysis routes for chemical recycling were assessed, glycolysis and methanolysis. Glycolysis was investigated as a depolymerisation route for PET bottles to recover its starting monomer - bis(2-hydroxyethyl) terephthalate (BHET), while methanolysis was applied to PC fraction to recover bisphenol A (BPA). Pyrolysis was assessed for degraded polyolefin-rich and polystyrene (PS) fractions to obtain hydrocarbon feedstocks.

The experimental results confirmed the feasibility of the investigated polymer-specific recycling pathways. Solvent-based recycling enabled high polymer recovery, reaching approximately 90–97%

for both, PP and HDPE, under the optimised conditions. PET glycolysis achieved ca. 76.9% BHET yield, while PC methanolysis enabled effective BPA recovery, with complete conversion achieved under selected catalytic conditions. Pyrolysis converted PE, PP and PS into hydrocarbon-rich products, with reaction temperature and catalyst type strongly influencing product distribution. Partner up-scale pyrolysis trials further demonstrated the feasibility of thermochemical conversion beyond laboratory scale, while also identifying the need for further optimisation of process control and product recovery. In practical terms, the results show that different fractions of ocean-bound plastic can be recovered as reusable polymers or valuable chemicals instead of being discarded.

Overall, the study confirms that successful management of river-collected OBP requires an integrated cascade approach combining sorting, cleaning, polymer identification and polymer-specific recycling. Mechanical recycling remains the preferred option for clean and homogeneous fractions, whereas solvent-based recycling offers additional value recovery for selected polyolefins. Chemical depolymerisation (solvolysis) provides efficient recovery of valuable chemical intermediates and monomers from condensation polymers such as PET and PC, while pyrolysis represents a potential complementary option for selected degraded or difficult-to-recycle polyolefin- and PS-rich fractions. Such a strategy maximises material recovery and supports the reintegration of collected OBP into circular economy.

# 1.
# Introduction

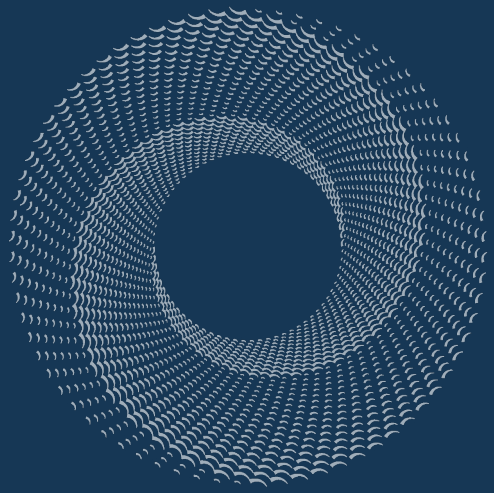

# 1. Introduction

## 1.1 Project Context and Scope

The Interreg South Baltic Circular Ocean-bound Plastic (COP) project, https://circularoceanplastic.eu/, is a cross-border initiative involving partners from Denmark, Poland, Germany, and Sweden. The project's mission is to identify challenges and opportunities for collecting, recycling, and reusing ocean-bound plastic waste in the region.

Within this framework, Work Package (WP) 4 focuses on the evaluation and development of recycling strategies for collected riverine plastic waste, including the assessment of its material composition, recycling potential, and suitability for advanced treatment technologies. This report presents the results of the chemical recycling investigations performed on plastic fractions collected from two pilot locations: the Motława River in Gdańsk (Poland) and the Aarhus River in Aarhus (Denmark). The recycling routes were selected according to the homogeneity, contamination level and degradation of the specific polymer fractions. By evaluating complementary recycling options, the study aimed to support an informed selection of recycling pathways based on the characteristics and condition of collected riverine plastic fraction. The work conducted within WP4 connects laboratory-scale recycling studies with recommendations for future waste valorisation pathways and the potential up-scaling of circular solutions for OBP management.

## 1.2 Challenges of Riverine Plastic

"Ocean-bound plastic" (OBP) refers to plastic waste located within proximity to coasts, in rivers, or in other waterways where there is a high probability of it entering the marine environment. OBP presents distinct technical challenges compared with standard post-consumer waste due to environmental degradation, organic contamination, and complex, multi-material construction (Ganzer et al., 2024). Prolonged exposure to ultraviolet (UV) radiation and moisture accelerates chemical weathering such as chain scission, oxidation, cracking, and discoloration, resulting in weakened quality and material performance. Additionally, riverine plastics typically carry substantial loads of dirt, residues, and biofilms, depending on their residence time in water. Finally, the high prevalence of multilayer packaging and composite items (e.g., bottles with caps and labels made from different polymers) makes conventional mechanical reprocessing impractical.

Despite these challenges, recycling OBP remains important because of the considerable amount of plastic waste already present in aquatic environments. An estimated 10–14 million tonnes of plastic enter the oceans annually, including approximately 1.6–2.4 million tonnes transported by rivers ;González-Fernández et al., 2022). Recycling these materials can recover part of their remaining

value, reduce reliance on virgin raw materials, and limit the amount directed to incineration or disposal. Moreover, mechanical recycling trials conducted within the Circular Ocean-bound Plastic (COP) project showed that riverine polypropylene (PP) could still be processed and used as a recycled material. However, its lower oxidative stability compared with virgin PP may restrict its use to less demanding applications or require blending with virgin material, additional stabilisation, and appropriate quality control (Mihut, 2026).

## 1.3 Background on chemical Recycling of Ocean-Bound Plastic

Chemical recycling represents a group of advanced technologies designed to address the limitations of traditional mechanical recycling, particularly for plastic waste recovered from aquatic and marine environments. While mechanical recycling is the preferred route for clean and homogeneous thermoplastics due to its technical simplicity and relatively low energy demand, its effectiveness may be limited for ocean-bound plastics exposed to prolonged UV radiation, oxidation, biofouling and mechanical forces. These factors can lead to chain scission, crosslinking, and the leaching of additives, resulting in a materials with more variable processing behaviour and reduced performance compared with virgin resins (Manzoor et al., 2022). In this context, chemical recycling potentially offers a complementary pathway by breaking down polymer chains into their original chemical building blocks, such as monomers, oligomers, or petrochemical fractions (hydrocarbons), using heat, chemical agents and/or solvents. This approach not only allows for the removal of organic contaminants and pigments but also enables the recovery of high-value raw materials that can be reintegrated into the circular economy to synthesise new polymers or chemicals (Gontarek-Castro et al., 2026). The general framework for plastic waste utilisation is presented in Figure 1.

The selection of a specific chemical recycling method depends primarily on the chemical structure of the polymer and its state of degradation. For polyolefins like polyethylene (PE) and polypropylene (PP), which dominate the OBP fractions found in riverine systems, thermochemical processes such as pyrolysis and gasification are most suitable. Pyrolysis involves the thermal decomposition of materials at high temperatures (typically between 300°C and 700°C) in an inert atmosphere, yielding liquid pyrolytic oils, gases, and waxes that can serve as feedstock for the petrochemical industry or be converted into synthetic fuels. For more complex or weathered polyolefin streams, catalytic cracking using zeolites like ZSM-5 can be employed to increase the yield of aromatic compounds and valuable gaseous fractions (Hou et al., 2021). For condensation polymers such as poly(ethylene terephthalate) (PET), polycarbonate (PC), and polyamides (PA), the preferred route is depolymerisation (solvolysis or chemolysis). This process uses specific cleaving agents to depolymerise the polymer under milder conditions than pyrolysis (Ragaert et al., 2017). A representative method is glycolysis, widely used for PET bottles, where a transesterification reaction with ethylene glycol (EG) produces the monomer

bis(2-hydroxyethyl) terephthalate (BHET). Similarly, methanolysis utilises methanol to break down PC or PET into their respective monomers, such as bisphenol A (BPA) and dimethyl terephthalate (DMT) (Datta & Kopczyńska, 2016).

Solvent-based recycling (often considered a physical method) provides a middle ground for purifying homogeneous but contaminated waste streams. This technique involves dissolving the target polymer in a selective solvent (such as xylene, toluene or green alternatives as cymene or limonene) to separate it from additives, dyes, and organic debris through filtration. The purified polymer is then recovered through precipitation or recrystallisation (Ibrahim et al., 2023).

Despite its potential, chemical recycling remains subject to debate. It has been recognised as a possible route for plastic fractions that are unsuitable for mechanical recycling, as it can recover monomers or produce hydrocarbon feedstocks (Harasymchuk et al., 2024). However, its environmental benefits are not guaranteed and depend strongly on the process, energy source, product yield and whether the recovered products replace virgin feedstocks or are used as fuels (Zhang & Nakatani, 2024). Several technologies are still developing towards commercial implementation, while high energy demand, process costs, feedstock contamination and the need for product purification remain primary limitations. Chemical recycling should therefore complement rather than replace mechanical recycling where the latter is technically feasible. Moreover, contaminated or mixed plastic waste may still require extensive sorting and pre-treatment; consequently, the suitability of chemical recycling should be assessed case by case within a broader hierarchy of recycling options (European Environment Agency, 2024).

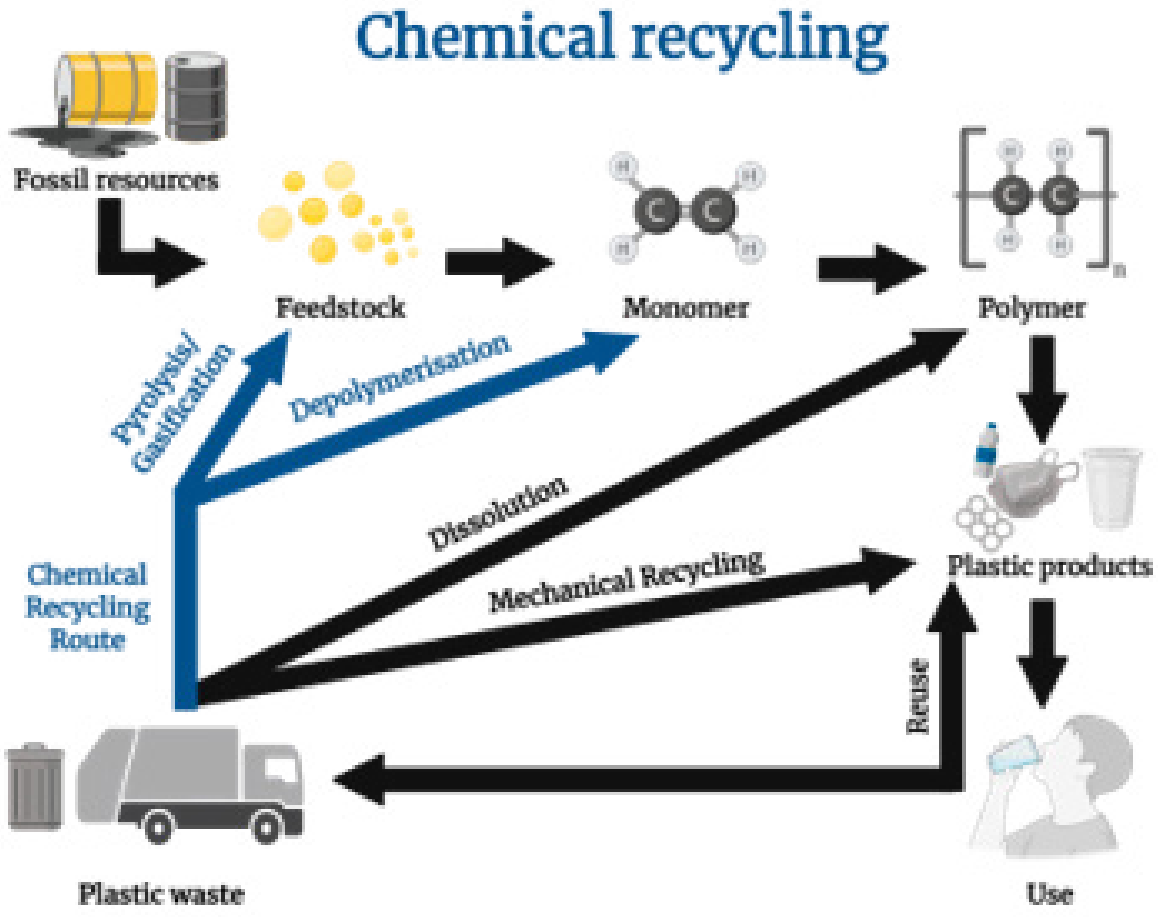


Fig. 1 Options for utilisation of plastic waste. Blue path is the chemical recycling route. Adapted from Plastics Europe (Plastics Europe, n.d.). Created with BioRender.com.

# 2.
# Materials selected for solvent-based and chemical recycling: OBP fractions from Aarhus and Gdańsk

# 2. Materials selected for solvent-based and chemical recycling: OBP fractions from Aarhus and Gdańsk

The materials investigated for chemical recycling were collected within the Interreg South Baltic project Circular Ocean-bound Plastic from two Baltic Sea rivers: the Motława River in Gdańsk (Poland) and the Aarhus River in Aarhus (Denmark). The collected fractions represent typical OBP, intercepted before entering the sea and therefore characterised by high variability in polymer composition, product origin, contamination level, and degree of environmental ageing.

The analysis of polymer composition (Polymer composition of river-collected plastic – Report, https://circularoceanplastic.eu/publication-polymer-composition-of-river-collected-plastic/ (Mihut et al., 2026) in Gdańsk and Aarhus reveals similarities, highlighting the common nature of riverine plastic pollution in the Baltic Sea region. In both locations, the waste stream is highly heterogeneous and dominated by plastics from the food and beverage packaging sectors. A shared feature is the dominance of three main polymer types: PE, PP, and PET, which reflects global plastic-production patterns and the widespread use of single-use items. Representative examples of the collected OBP fractions are shown in Figure 2.

In Gdańsk (Motława River), these three fractions account for 91% of identified items, with PE at 34%, PET at 30%, and PP at 27%. Polystyrene (PS) was also identified as a notable fraction in Gdańsk, accounting for 4% of the total items, primarily in the form of polystyrene foam and small containers.

Similarly, in Aarhus (Aarhus River), polyolefins and PET remain dominant, though with a different internal distribution: PP (43%), PE (33%), and PET (11%), alongside a significant polycarbonate (PC) fraction of 14%. In this location, PS represents a minor portion of the waste stream (less than 1% by weight).

The most significant technological challenge shared across both collection sites is the physicochemical condition of the collected plastics. OBP from Gdańsk and Aarhus was consistently “raw” and untreated, contaminated with organic matter, saturated with moisture, and characterised by a strong river odour. Moreover, the PS and PET fractions clearly displayed environmental degradation like discoloration, brittleness, and fragmentation (Figure 2). These issues of contamination, heterogeneity and degradation can substantially limit mechanical recycling and increase the need for additional approaches, such as chemical and solvent-based recycling explored in the COP project.


Fig. 2 Examples of collected raw OBP fractions from Aarhus and Gdańsk.

Based on the polymer identification and visual assessment of the collected materials, specific fractions were selected as candidates for chemical and solvent-based recycling pathways. The selection was guided by polymer structure and expected degradation behaviour:

- Polyolefin fractions (PP and PE): mainly originating from rigid packaging, caps, lids, cups, and flexible packaging. These materials represent the largest fraction of collected OBP; however, their heterogeneous composition and possible ageing limit direct mechanical recycling. For selected cleaner fractions, solvent-based purification can be considered, while more degraded or mixed polyolefin streams may require thermochemical conversion routes such as pyrolysis.
- PS: originated from plastic cup lids and expanded PS (Styrofoam).
- PET fractions: mainly originating from beverage bottles. Due to the condensation polymer structure of PET, chemical depolymerisation through solvolysis routes, particularly glycolysis, provides an opportunity to recover valuable monomers such as bis(2-hydroxyethyl) terephthalate (BHET).
- PC fractions: identified mainly in the Aarhus collection stream. Due to its condensation polymer structure, chemical recycling through solvolysis as methanolysis can enable recovery of valuable chemical building blocks, including bisphenol A (BPA).
- Complex and highly contaminated fractions: including multilayer packaging, mixed polymer products, and strongly degraded materials. These fractions represent the most challenging part of the OBP stream and are considered unsuitable for conventional recycling without advanced treatment

Figure 3 presents the workflow applied within the COP project, from collection and polymer identification to the selection of recycling pathways and product recovery.

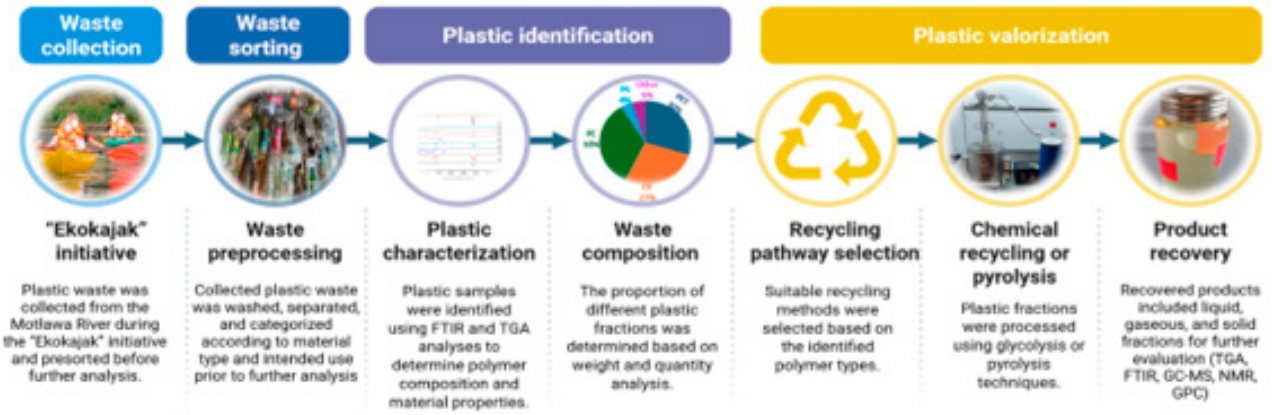


Fig. 3 Workflow for the collection, sorting, polymer identification, recycling-pathway selection, chemical recycling and recovery of products from OBP within the COP project. Created with BioRender.com.

The analysed OBP materials represent a challenging but potentially valuable secondary raw material stream. Their heterogeneous nature prevents the application of a single recycling solution; instead, an integrated approach combining sorting, cleaning and polymer-specific treatment is required. Therefore, complementary recycling pathways were investigated. The selection of a specific recycling route was based on the chemical structure, contamination level and degree of degradation of each plastic fraction (Table 1). This approach provides a more informed basis for identifying the most appropriate recycling route rather than assuming that a single technology is suitable for all collected plastics.

Table 1 Overview of OBP fractions considered for chemical recycling

| Polymer | Main OBP source | Condition | Selected route |
|---|---|---|---|
| PP | Cups | Relatively clean rigid fraction | Mechanical / solvent-based recycling/ pyrolysis |
| HDPE | Caps, bags | Depends on contamination | Solvent-based recycling/ pyrolysis |
| LDPE | Foil, bags | Contamination and degradation possible | Pyrolysis |
| PS | Styrofoam | Contamination and degradation possible | Pyrolysis |
| PET | Bottles | Contamination and degradation possible | Glycolysis (solvolysis) |
| PC | Reusable cups | Relatively clean fraction | Methanolysis (solvolysis) |

# 3.
# Solvent-based and chemical recycling options for OBP

# 3. Solvent-based and chemical recycling options for OBP

The chemical recycling investigations were evaluated in relation to the polymer composition, contamination level, and degradation state of the OBP fractions collected within the COP project. Like the assessment performed for mechanical recycling, the suitability of each recycling pathway was determined not only by polymer identification but also by the quality and expected processability of the recovered material stream.

## 3.1 Green solvent-based recycling of polyolefins

The solvent-based approach was evaluated for relatively homogeneous polyolefin fractions, particularly PP and high-density polyethylene (HDPE). The purpose was to determine whether dissolution–precipitation using sustainable "green" solvents can selectively purify polyolefins, remove pigments and additives, and recover polymer powders with structural and thermal properties comparable to virgin materials.

The affinity of selected green solvents towards PP is presented in Figure 4 using the Hansen solubility parameter sphere. Green solvents (p-cymene, limonene, formaldehyde dibutyl acetal (FDBA)) were selected due to their lower toxicity, bio-origin, and favourable Hansen solubility parameters for polyolefins as sustainable alternatives to xylene.

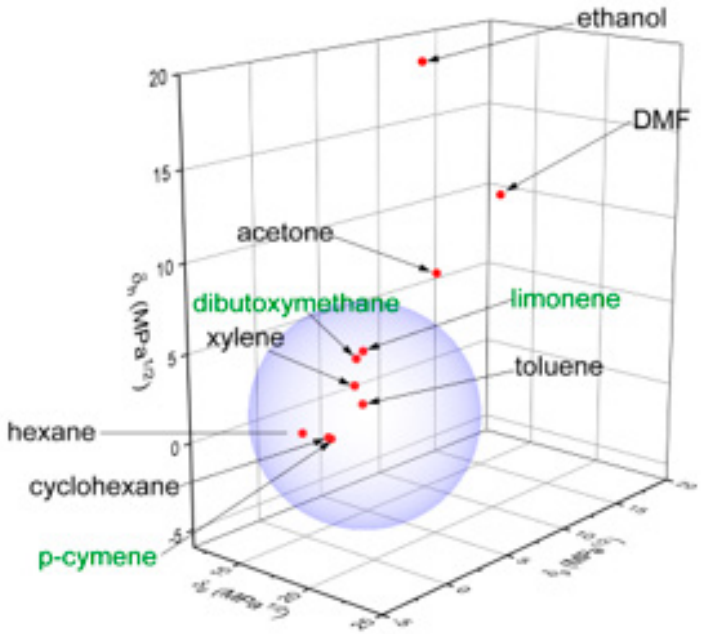


Fig. 4 Hansen Solubility Parameters (HSP) sphere for PP, illustrating the affinity of green solvents as sustainable substitutes for conventional solvents

### 3.1.1 Experimental set-up

Polyolefin fractions (PP cups and HDPE bottle caps, shown in Figure 2) were selected based on polymer identification results and their relatively homogeneous composition. Small pieces of cut or ground polymer were placed in a flask with the selected green solvent and heated at the specified temperature for 30 min to achieve dissolution. After this period, the hot polymer solution was poured into the antisolvent (ethanol), which induced rapid precipitation of the polymer and facilitated the separation of soluble additives and contaminants.

The mixture was stirred for several hours to ensure complete precipitation, after which the polymer was filtered and dried. The experimental matrix included variations in solvent type, dissolution temperature (90–130 °C), polymer concentration (5 wt.% vs. 10 wt.%), and solvent-to-antisolvent volume ratios (1:2, 1:4, 1:8) to identify optimal conditions for high-quality polymer recovery. Figure 5 illustrates the steps of the dissolution-precipitation process.

Recovered powders were dried and characterised using:

- visual observation of the formed powder;
- Fourier-transform infrared (FTIR) spectroscopy – to assess chemical integrity, detect oxidation, and evaluate changes in crystallinity;
- Differential Scanning Calorimetry (DSC) analysis – to determine melting behaviour, crystallisation temperature and apparent crystallinity relative to starting material.

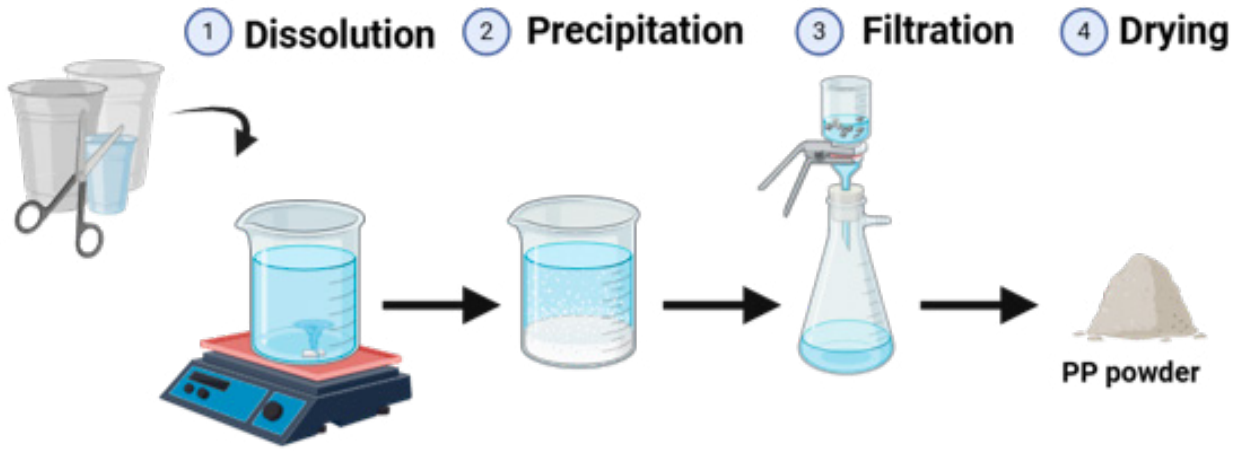


Fig. 5 Set-up for solvent-based recycling of PP or HDPE.

### 3.1.2 Solvent-based recycling of HDPE

HDPE bottle caps were used as the starting material, representing a relatively homogeneous fraction, though variable in colour. For these solvent-based reactions, we tested different variables to evaluate changes in the material, including: the type of solvent, the reaction temperature (90, 110, and 130 °C), the concentration of the polymer in the solvent (5-10 wt.%), and the volume ratio of added antisolvent (1:2, 1:4, and 1:8). All samples exhibited a high recovery rate of approximately 93-99%.

#### 3.1.2.1 Visual observation

The influence of solvent type and dissolution temperature on recovered HDPE morphology is summarised in Table 2. Processing at 90 °C only resulted in a surface wash of impurities without dissolving the polymer. Full dissolution and subsequent precipitation of powder were achieved at temperatures between 110 °C and 130 °C.

Table 2 Effect of solvent type and processing temperature on the visual morphology of recovered HDPE from bottle caps.

| Sample | Conditions (solvent, concentration, T, solvent :EtOH) | Form | Comment |
|---|---|---|---|
| HDPE_cym_90 | Cymene; 5%; T=90 oC; 1:8 |  | No melting observed; the material was only superficially washed. |
| HDPE_cym_110 | Cymene; 5%; T=110 oC; 1:8 |  | Homogeneous solution achieved; successful material recovery. |
| HDPE_cym_130 | Cymene; 5%; T=130 oC; 1:8 |  | Homogeneous solution achieved; successful material recovery. |

| | | | |
|---|---|---|---|
| HDPE_lim_130 | Limonene; 5%; T=130 oC; 1:8 |  | Homogeneous solution achieved; successful material recovery. |
| HDPE_ FDBA_130 | FDBA; 5%; T=130oC; 1:8 |  | Homogeneous solution achieved; successful material recovery. |
| HDPE_xyl_130 | Xylene; 5%; T=130oC; 1:8 |  | Full dissolution was achieved, but severe agglomeration occurred during precipitation, which is consistent with aromatic solvent behaviour. |
| HDPE_cym_10% | Cymene; 10%; T=130 oC; 1:8 |  | Very viscous solution; the polymer did not completely dissolve within the reaction time, and other fractions remained visible. High viscosity limited effective precipitation. |
| HDPE_cym_1:2 | Cymene; 5%;, T=130 oC; 1:2 |  | Homogeneous solution formed, but the antisolvent volume was too low to properly induce powder precipitation. Insufficient ethanol volume resulted in incomplete precipitation and block formation. |

### 3.1.2.2 FTIR analysis

The FTIR spectra of the recovered HDPE powders show the typical polyethylene bands at 2920 and 2850 cm $^{1}$ ($CH_2$ stretching), 1465 cm $^{1}$ ($CH_2$ bending), and ~721 cm $^{1}$ ($CH_2$ rocking), confirming that the polymer backbone remains chemically intact after the dissolution-precipitation process, as shown in Figure 6.

This indicates that solvent-based recycling does not alter the primary chemical structure of the polymer. Also, no absorption band was detected in the carbonyl region (1715–1730 cm $^{1}$), suggesting that no measurable oxidative degradation occurred during processing at selected dissolution temperatures

(90–130 °C) and solvents did not promote significant oxidation or chain scission. Although, in general the spectra of all recovered powders are similar, minor differences can be observed in the fingerprint region (800–1200 cm $^{1}$), which may be related to differences in chain packing and crystalline morphology resulting from dissolution and reprecipitation.

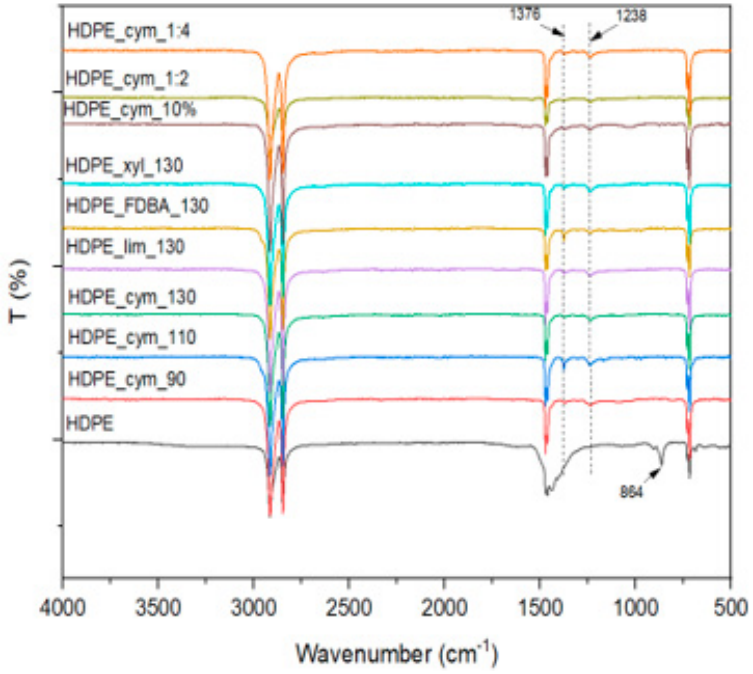


Fig. 6 FTIR spectra of recovered powders from HDPE solvent-based recycling.

### 3.1.2.3 DSC analysis

DSC melting peaks (Tm) for recovered HDPE ranged between 129 °C and 135 °C (Figure 7). While slightly lower than the starting feedstock (138.8 °C), these values remained stable across all tested solvents, indicating that thermal processing did not cause severe chain scission, in agreement with FTIR analysis. Crystallisation temperature (Tc) values (110–117 °C) reflect the typical crystallisation behaviour of HDPE after solvent processing (Table 3). Crystallinity values (55–65%) match HDPE ranges reported in the literature (Tarani et al., 2023). Notably, p-cymene at 130 °C produced material with the highest crystallinity (64.2%), outperforming traditional xylene (56.3%) and FDBA (55.9%). This shows that the processing conditions can influence the final material properties.

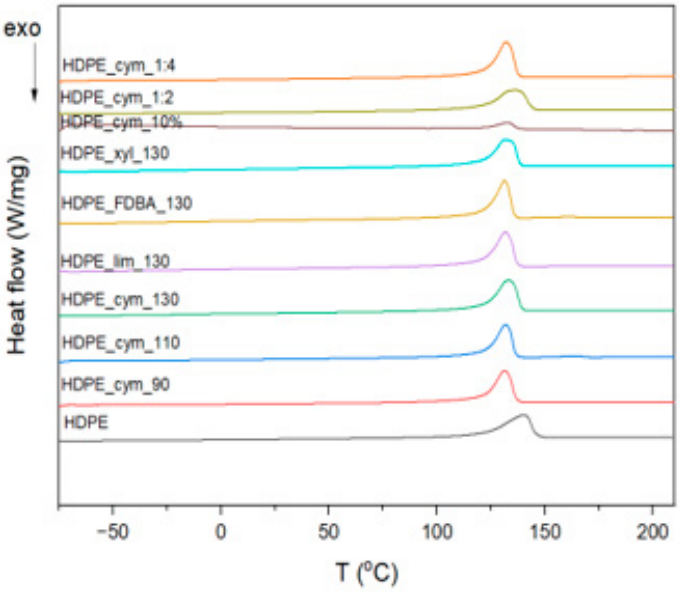


Fig. 7 DSC melting curves of recovered HDPE.

Table 3 Thermal properties (DSC) of recovered HDPE powders.

| Sample | Tm (oC) | Tc (oC) | ΔH (J/g) | Xc (-) |
|---|---|---|---|---|
| HDPE | 138.8 | 110.0 | 148.6 | 50.72 |
| HDPE_cym_90 | 132.7 | 112.7 | 152 | 51.88 |
| HDPE_cym_110 | 131.8 | 116.1 | 131.8 | 44.98 |
| HDPE_cym_130 | 133 | 114.5 | 188.1 | 64.2 |
| HDPE_lim_130 | 130.3 | 116.0 | 176.6 | 60.3 |
| HDPE_FDBA_130 | 132.1 | 116.5 | 163.9 | 55.9 |
| HDPE_xyl_130 | 129.4 | 114.1 | 165.1 | 56.3 |
| HDPE_cym_10% | 133.9 | 114.4 | 30.82 | 10.52 |
| HDPE_cym_1:2 | 135.6 | 110.6 | 168 | 57.3 |
| HDPE_cym_1:4 | 132.2 | 115.8 | 180.6 | 61.64 |

### 3.1.2 Solvent-based recycling of HDPE

PP cups were subjected to solvent-based recycling as an alternative valorisation route alongside mechanical recycling done by Plast Center Denmark ("Mechanical tests &material analysis on recycled samples"; https://circularoceanplastic.eu/publication-mechanical-performance-of-recycled-ocean-bound-plastic/).

The parameters such as type of green solvents: p-cymene, limonene and FDBA and dissolution temperatures between 90 and 130 °C were tested. These solvents enabled dissolution of PP and subsequent recovery of purified polymer powder from contaminated OBP streams.

#### 3.1.3.1. Visual observation

The reaction temperature is crucial. Figure 8 provides a visual summary of material morphology recovered from different solvents processed at different temperature ranges. When lower temperatures (90–110 °C) were used, no homogeneous solution was formed, and the PP flakes remained floating intact in the mixture. At 120 °C, initial optical changes were observed (for PP_cym and PP_FDBA), making the material appear opaquer and more swollen. Full dissolution occurred at 130 °C, enabling clean phase separation and high-quality powder precipitation upon cooling and drying.


Fig. 8 Effect of solvent type and processing temperature on the visual morphology of PP.
Reaction conditions: 5% of polymer, 90-130 °C, time:30 min, solvent to antisolvent volume 1:8.

### 3.1.3.2. FTIR analysis

To assess structural changes induced by the process, FTIR analysis was performed. The FTIR spectra of the recovered PP powders from the green solvents exhibit characteristic bands of PP, such as the $CH_3$ asymmetric and symmetric stretching vibrations at ~2960 $cm^{-1}$ and ~2870 $cm^{-1}$, and the characteristic $CH_3$ bending vibration at ~1380 $cm^{-1}$, confirming preservation of the polymer backbone during dissolution-precipitation process (Figure 9).

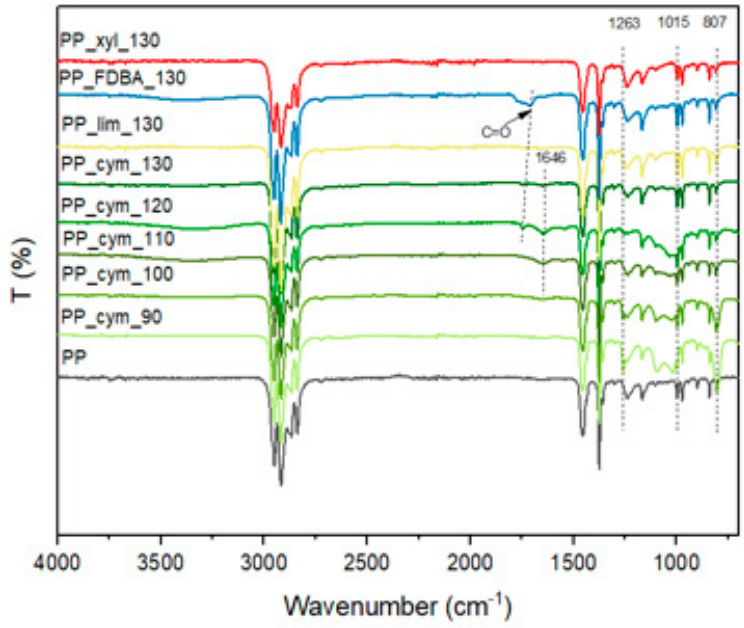


Fig. 9 FTIR spectra of recovered powders from PP solvent-based recycling.

### 3.1.3.2. FTIR analysis

To assess structural changes induced by the process, FTIR analysis was performed. The FTIR spectra of the recovered PP powders from the green solvents exhibit characteristic bands of PP, such as the $CH_3$ asymmetric and symmetric stretching vibrations at ~2960 cm $^{1}$ and ~2870 cm $^{1}$, and the characteristic $CH_3$ bending vibration at ~1380 cm $^{1}$, confirming preservation of the polymer backbone during dissolution-precipitation process (Figure 9).

Crystallinity-sensitive absorptions at ~1015 cm $^{1}$ and ~807 cm $^{1}$ are present in all recovered fractions, but their relative intensities vary with processing temperature. Samples treated at elevated temperatures (120–130 °C) show the highest changes from the reference PP spectrum, consistent with temperature-driven changes in the crystalline–amorphous balance. This correlates with the observed loss of optical clarity in the recovered PP. In contrast to HDPE, which showed no carbonyl activity across all tested temperatures, PP exhibits higher thermal-oxidative sensitivity. At 130 °C (and at 120 °C for FDBA), weak but distinct absorptions emerge in the carbonyl region (1710–1740 cm $^{1}$), indicating the onset of oxidation.

This behaviour is consistent with early PP oxidation pathways involving hydroperoxide formation and subsequent carbonyl-containing species. The susceptibility arises from the presence of tertiary carbon atoms along the PP backbone, which serve as favourable sites for radical generation and oxygen attack under thermal stress. The broad band at 1646 cm-1 for sample PP_FDBA_130 may originate from residual solvent/antisolvent or formation of C=C due to degradation. Overall, FTIR analysis demonstrates that solvent-based recycling preserves the primary chemical structure of PP,

with temperature-dependent recrystallisation and limited oxidation.

Carbonyl index (CI) was calculated as the deviation of maximum peak of 1715 cm-1 to maximum absorbance band of 1455 cm-1 for each sample (Figure 10).

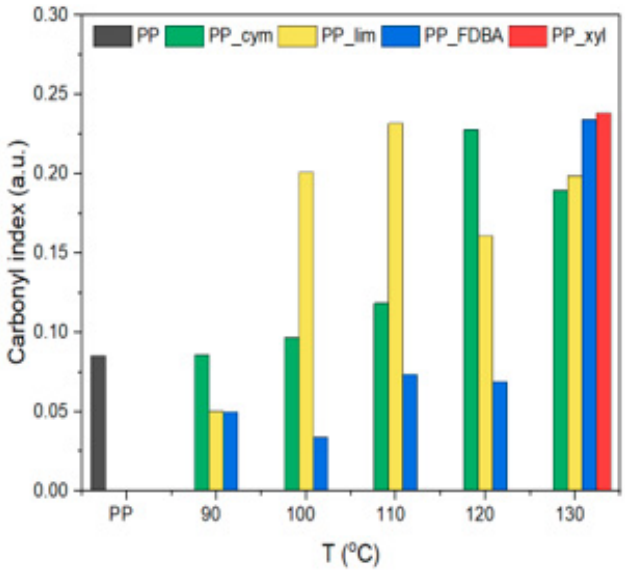


Fig. 10 Carbonyl index of recovered PP as a function of temperature and solvent type.

The carbonyl index data further corroborate the FTIR observations. Increasing processing temperature leads to a systematic rise in carbonyl formation across all solvent systems, confirming temperature-driven initiation of oxidation. Among the tested solvents, limonene shows the fastest onset of carbonyl development, with a clear increase already at 100oC. PP processed in cymene maintains low carbonyl levels up to ~110 °C, while PP recovered from FDBA remains chemically stable up to ~120 °C, indicating a slightly higher resistance to early oxidation in this solvent environment.

### 3.1.3.3 DSC analysis

For the successfully dissolved PP samples at 130 °C, thermal properties remained relatively stable, confirming that the short-term dissolution process did not induce severe thermal degradation (Table 4).

Table 4 Thermal properties (DSC) of recovered PP powders

| Sample | Tm (oC) | Tc (oC) | ΔH (J/g) | Xc (%) |
|---|---|---|---|---|
| PP | 167.3 | 124.5 | 83.22 | 40.20 |
| PP_cym_130 | 166.3 | 124.7 | 73.85 | 35.3 |
| PP_lim_130 | 161.2 | 122.6. | 51.51 | 24.6 |
| PP_FBDA_130 | 158.1 | 121.2 | 47.64 | 22.8 |
| PP_xyl_130 | 163.6 | 125.3 | 72.99 | 34.9 |

However, a shift towards lower melting temperature is observed, from 168 °C for the starting PP to 158 °C for PP recovered using FDBA (PP_FDBA_130) (Figure 11).

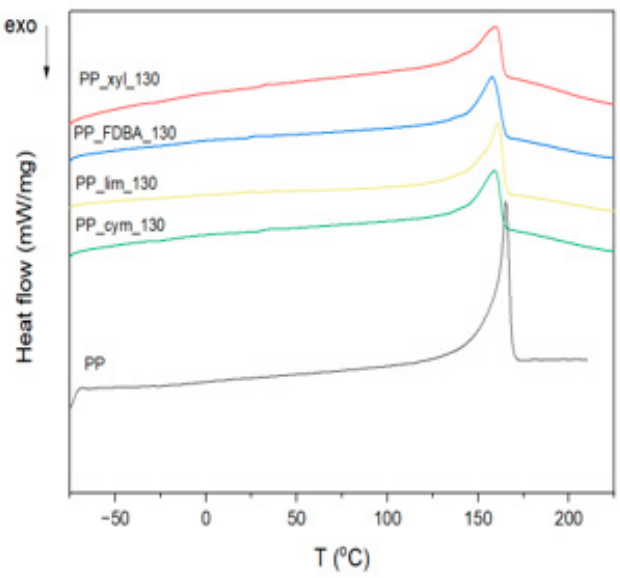


Fig. 11 DSC melting curves of recovered PP powders.

Green solvents influenced the final morphology. Cymene-recovered PP exhibited the highest crystallinity (35.3%), suggesting a solvent-induced crystallisation effect that promotes more orderly chain packing compared to limonene or FDBA. The crystallinity calculation was based on a reference melting enthalpy of 209 J/g for 100% crystalline isotactic PP. When correlated with the DSC data, these structural changes explain the sharp decline in crystallinity observed in FDBA and limonene matrices (dropping to 22.8% and 24.6%, respectively), as the newly formed oxygenated groups disrupt regular chain packing. These results indicate that processing temperature should be carefully controlled, particularly for PP, where initial oxidation was observed at higher temperatures. The use of stabilisers or an inert atmosphere could therefore be considered in further optimisation of the process.

### 3.1.4 Summary

FTIR and DSC analyses confirmed that, when excessive thermal degradation was avoided, the recovered resins retained their characteristic chemical and thermal behaviour. For both HDPE and PP, p-cymene at 130 °C yielded the highest crystallinity out of all tested solvents, outperforming traditional hazardous xylene. Using xylene on HDPE caused the recovered powder to agglomerate heavily during precipitation. Furthermore, reducing the antisolvent (ethanol) volume ratio down to 1:2 resulted in incomplete precipitation, establishing 1:8 as the optimal ratio.

The recovered powders could be further processed by compounding or extrusion, although their molecular weight, mechanical properties and long-term stability should first be evaluated. Notably, the possible PP oxidation should be considered with addition of stabilisers. This is also in agreement with the results from the report on "Mechanical tests &material analysis on recycled samples", https://circularoceanplastic.eu/publication-mechanical-performance-of-recycled-ocean-bound-plastic/, where PP revealed oxidation after processing (Mihut, 2026).

**Practical implications**

The obtained results demonstrate that solvent-based recycling is particularly suitable for relatively clean and homogeneous polyolefin fractions collected from rivers. Besides recovering the polymer itself, the process enables partial removal of pigments, additives and surface contaminants, resulting in improved material quality compared with direct mechanical recycling. However, efficient application of this technology requires prior sorting and polymer-specific separation, limiting its applicability for highly mixed waste streams.

## 3.2 Glycolysis of PET

Although PET bottles are generally considered suitable for mechanical recycling, the PET fraction collected during the EkoKayak initiative (Figure 2) showed a high degree of environmental degradation and contamination, including discoloration, cracking, and material embrittlement. Given these limitations, glycolysis was evaluated as a chemical recycling route for collected PET waste.

Glycolysis enables the depolymerisation of PET through transesterification with ethylene glycol (EG), resulting in the formation of lower-molecular-weight oligomers and the monomer bis(2-hydroxyethyl) terephthalate (BHET).

The study focused on the optimisation of reaction parameters (reaction time, temperature, EG/PET ratio), as well as on the evaluation of different catalytic systems. In addition to the conventional homogeneous catalyst zinc acetate, novel heterogeneous magnetic catalysts based on cobalt spinel

ferrite supported on zeolites were investigated.

### 3.2.1. Experimental set-up

Prior to the reaction, the PET bottles were subjected to a standardised preparation procedure: shredding grinding cleaning drying. The preparation procedure was designed to minimise the influence of surface contamination and moisture on the glycolysis process, ensuring that the observed results primarily reflected the intrinsic reactivity of the recovered PET. Cleaning was performed using 1 M NaOH with agitation, based on earlier project recommendations (Pathways for Cleaning Collected Ocean-bound Plastic, https://circularoceanplastic.eu/report-pathways-for-cleaning-collected-ocean-bound-plastic) (Gontarek-Castro et al., 2025).

Glycolysis reactions were carried out in a round-bottom flask equipped with a reflux condenser and magnetic stirring (Figure 12). In a typical experiment, 2.5 g of PET flakes were mixed with 19.5 g of ethylene glycol (EG), corresponding to an EG/PET molar ratio of approximately 24. The reaction mixture was heated to the set temperature (185, 197 or 200 °C) and held for 90 min. Zinc acetate (Zn(OAc)2) a catalyst commonly used in PET glycolysis, was selected and used at 1 wt.% relative to PET (Kosloski-Oh et al., 2021). After completion of the reaction, the mixture was cooled and mixed with 50 mL of boiling water and filtered to remove any remaining insoluble residues (oligomers). The filtrate was stored at 4 °C overnight to promote BHET crystallisation. The obtained white needle-like BHET crystals were collected by vacuum filtration, washed with cold deionised water, and dried at 40-60 °C.

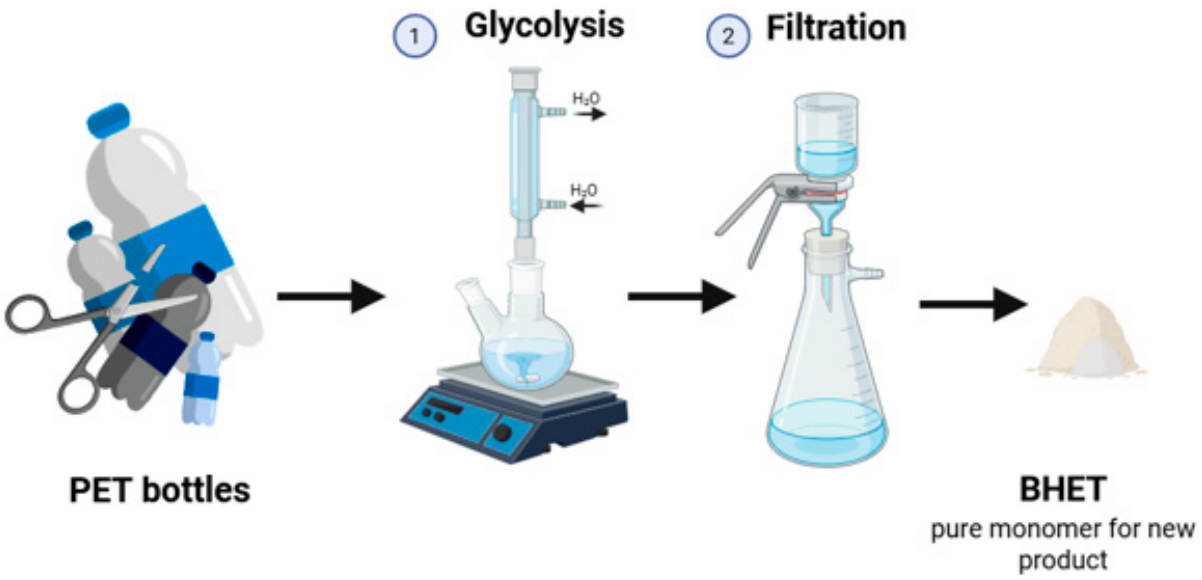


Fig. 12 Set-up for glycolysis of PET to obtain BHET.

To evaluate the efficiency of the glycolysis reaction, two parameters were monitored:

- PET conversion, defined as the complete dissolution of PET flakes within the specified reaction time, and
- BHET yield (YBHET), calculated as:

$$Y_{BHET} = \frac{m_{BHET}}{m_{PET} * \frac{M_{BHET}}{M_{PET}}} x100\%$$

Where MBHET=254.24 g/mol MPET repeat unit=192.17 g/mol

The recovered BHET monomer was subsequently characterised using:

- FTIR spectroscopy
- thermogravimetric analysis (TGA).

These analyses were performed to confirm the chemical structure and assess the thermal stability of the recovered monomer.

### 3.2.2. Glycolysis reaction optimisation

To achieve satisfactory monomer yields, the reaction conditions were systematically optimised by varying the EG/PET mass ratio (4.7-20), reaction temperature (185-200 °C), and reaction time (60-90 min) (Figure 13). The optimisation experiments enabled the identification of the most favourable conditions for BHET production and highlighted the importance of maintaining appropriate stoichiometric ratios between EG and PET to maximise monomer yield.

**Effect of EG/PET mass ratio**

The EG/PET mass ratio had a significant impact on the efficiency of depolymerisation. As shown in Figure 13a, increasing the EG/PET ratio from 4.7 to 7.3 resulted in an increase of BHET yield, but further increasing the EG/PET ratio to 10.3 and 20.3 led to a gradual decrease in BHET yield. The optimum was found at an EG/PET mass ratio of approximately 7.3–7.5 (corresponding to a molar ratio of about 24).

**Effect of reaction time**

Reaction time strongly influenced BHET formation (Figure 13b). Extending the reaction duration from 60 to 90 minutes led to a systematic increase in BHET yield, rising from 43.24% to 66.69%. This trend confirms that longer exposure to glycolysis conditions promotes more complete cleavage of ester bonds within the PET structure. A reaction time of 90 minutes provided the highest yield within the

tested range.

### Effect of temperature

Temperature was identified as a critical parameter governing depolymerisation kinetics (Figure 13c). Increasing the temperature from 185°C to 197°C significantly enhanced BHET yield, reaching a maximum of 76.9%. A further increase to 200°C resulted in a slight decrease in yield, suggesting that excessively high temperatures may promote side reactions or retransesterification back to oligomers. Therefore, the reflux temperature of ethylene glycol (197°C) was selected as the optimum operating temperature for PET glycolysis under the investigated conditions.

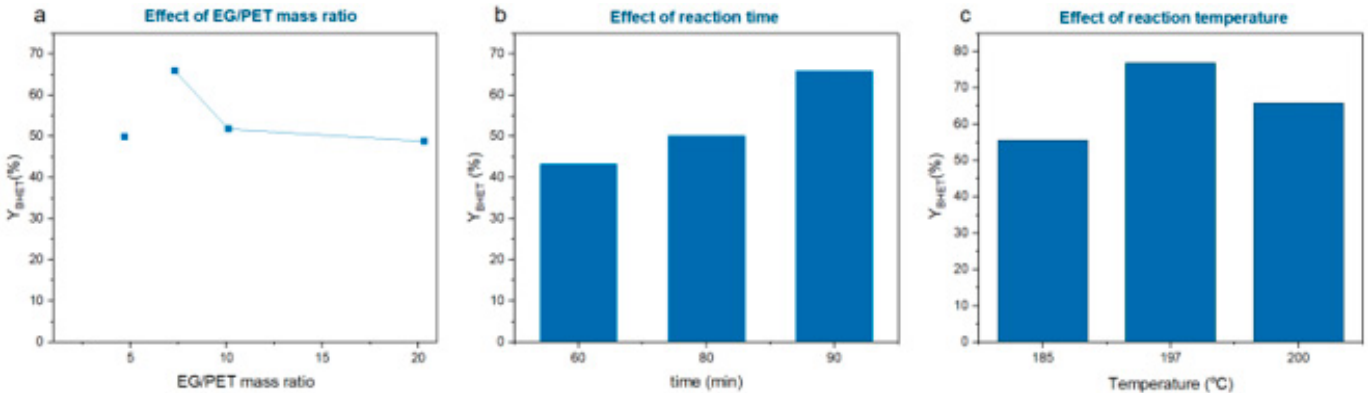


Fig. 13 Optimisation of PET glycolysis: a) EG/PET ratio, b) time, c) temperature

The optimised conditions were subsequently applied in a larger laboratory-scale experiment, increasing the PET feed from approximately 1–2 g to 25 g, corresponding approximately to the amount of PET contained in a 1.5 L bottle (excluding the cap and bottom section). Under the optimised reaction conditions, the scaled-up process achieved a BHET yield of 78.2%, closely matching the yield obtained at a smaller scale (76.9%). These results indicate that the optimised reaction conditions can be transferred to a larger laboratory batch without a substantial loss in depolymerisation efficiency. Further pilot-scale studies are required to assess process scalability under continuous or larger-batch operating conditions.

### Effect of magnetic catalysts

Although homogeneous catalysts such as zinc acetate are highly effective and widely used for PET glycolysis, they are difficult to separate from the reaction mixture, often resulting in catalyst loss and contamination of the recovered products. Consequently, heterogeneous catalysts represent an attractive alternative (Mark et al., 2020).

As a more sustainable approach, we proposed magnetic catalysts for PET glycolysis, particularly spinel ferrites ($CoFe_2O_4$, also referred as CFO), because they can be rapidly separated using an

external magnetic field (Yun et al., 2023). Supporting the spinel ferrites on porous materials like ZSM-5 zeolite can enhance their catalytic performance by providing a higher surface area and increasing the exposure of active Lewis's acid sites. The catalysts were prepared in two steps. First spinel ferrites were obtained from precursors and then spinel ferrites and ZSM-5 were ground together in an agate mortar until homogeneous. Composites were prepared at different mass ratios: 90/10, 75/25, 60/40, 50/50, and 25/75 (CFO/ZSM-5). The mixtures were placed in ceramic crucibles and calcined in air at 400°C.

The glycolysis of river-recovered PET bottles was performed at optimised conditions: 197°C for 90 minutes with an EG/PET mass ratio of 7.5. The catalytic performance of the CFO/ZSM-5 composites varied with the ferrite-to-zeolite ratio (Figure 14). The highest BHET yield of 69.1% was achieved using the CFO/ZSM-5 (75/25) catalyst. For comparison, pure CFO yielded 60.7%, while a blank test (no catalyst) resulted in only 22.7% yield. Interestingly, pure ZSM-5 showed no catalytic activity (0% yield), confirming that the ferrite species provide the primary active sites for the transesterification reaction.

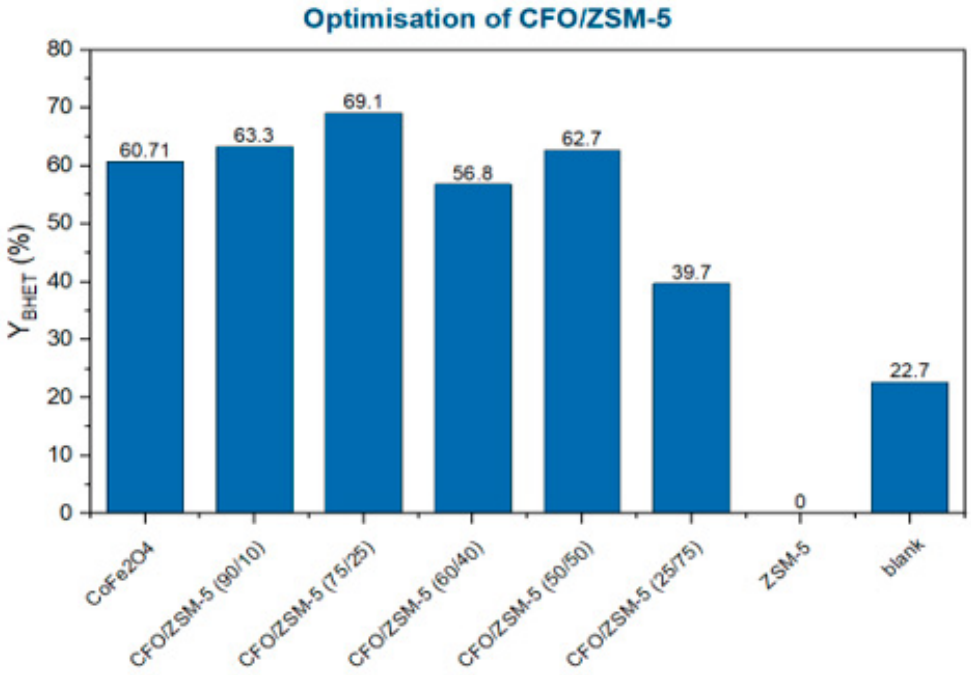


Fig. 14 PET glycolysis efficiency using magnetic catalysts

The catalyst was separated via an external magnet (Figure 15). Prior to magnetic separation, a small amount of warm methanol was added to the post-reaction mixture to facilitate separation. The catalyst was observed to settle within 2–3 minutes, allowing for rapid decantation of the liquid phase.

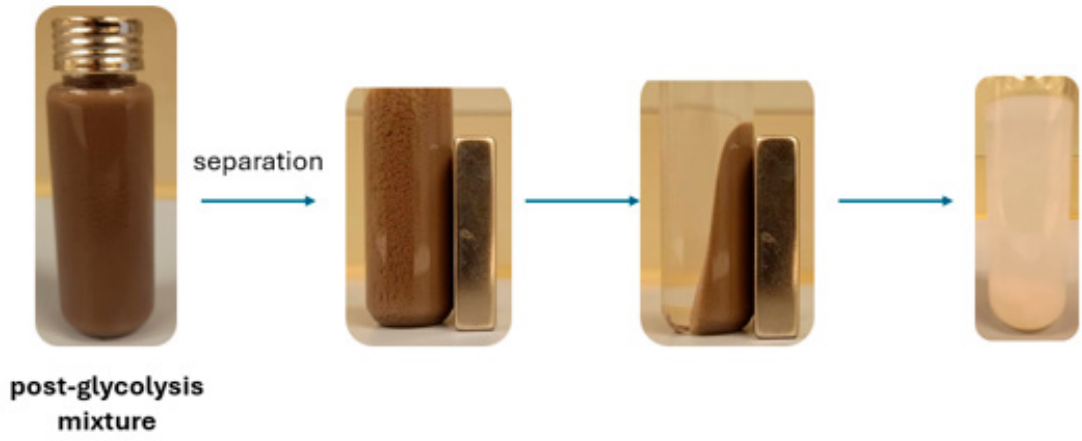


Fig. 15 Separation of the magnetic catalyst from the post-glycolysis mixture using an external magnet

Reusability tests for the CFO/ZSM-5 (75/25) catalyst in PET glycolysis showed a gradual decrease in BHET yield over consecutive cycles. The yield dropped from 69.1% in the first cycle to 45.5% in the second, and 39.6% in the third. This decrease is partially attributed to the handling process and the partial solubility of the monomer in the methanol used during the cleaning steps.

Additionally, potential loss of catalyst during cleaning and blockage of active sites by adsorbed oligomers might contribute to the deactivation, a phenomenon commonly observed in heterogeneous PET recycling systems. Despite the gradual decrease in activity, the catalyst remained catalytically active after three consecutive cycles, demonstrating the feasibility of catalyst recovery and reuse.

### 3.2.3 FTIR analysis of BHET

FTIR was used to confirm the chemical structure of the recovered BHET and to compare products obtained from different PET feedstocks (e.g., different bottle colour) and catalytic systems. Figure 16 presents the FTIR spectra of BHET obtained from green and blue PET bottles, BHET produced in the blank reaction (no catalyst), BHET synthesised using $Zn(OAc)_2$ and CFO/ZSM-5 (75/25), as well as spectra of the oligomeric fraction and reference PET.

The PET spectrum displays a strong C=O band at ~1715 $cm^{-1}$, characteristic aromatic bands at 1500–1600 $cm^{-1}$, and absence of the broad O–H band, reflecting the polymeric nature and lack of terminal hydroxyl groups. Comparison with BHET spectra clearly demonstrates the cleavage of ester bonds and formation of monomeric products. All BHET samples exhibit the characteristic vibrational bands expected for BHET: broad O–H stretching band at ~3400 $cm^{-1}$, confirming the presence of terminal hydroxyl groups; strong ester C=O stretching at 1715–1725 $cm^{-1}$, aromatic C=C stretching at 1500–1600 $cm^{-1}$, corresponding to the benzene ring of the terephthalate core and C–O–C and C–O stretching bands in the 1100–1250 $cm^{-1}$ region, associated with the ethylene glycol moieties.

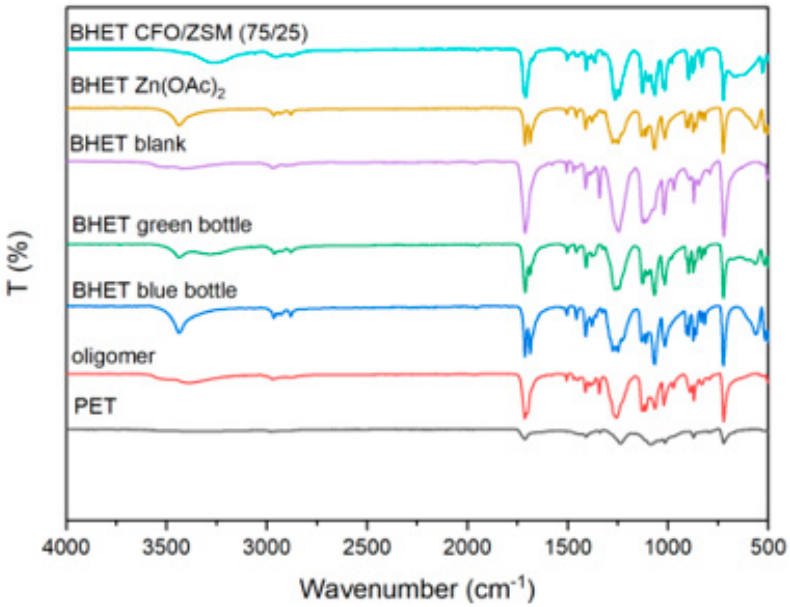

Fig. 16 FTIR spectra of PET and PET glycolysis products (oligomer and BHET)

- The spectra obtained for BHET recovered from green and blue PET bottles shows spectra fully consistent with pure BHET, indicating that colorants and environmental ageing do not alter the chemical structure of the recovered monomer.
- The BHET spectrum from the blank reaction displays the same characteristic BHET bands, but with lower peak intensities and slightly broader features, consistent with the lower BHET yield and the probable presence of residual oligomers. The C=O band is less sharp, indicating incomplete depolymerisation.
- The $Zn(OAc)_2$ sample shows well-defined ester and aromatic bands, indicating high monomer purity.
- BHET obtained using the CFO/ZSM-5 (75/25) catalyst exhibits spectra nearly identical to the $Zn(OAc)_2$ sample, confirming that the heterogeneous magnetic catalyst produces BHET of comparable structural purity to zinc acetate. No additional bands associated with ferrite or zeolite residues are observed, demonstrating effective magnetic separation.

The oligomer spectrum shows a broader and slightly shifted C=O band, reduced O–H stretching intensity, and stronger contributions in the 1100–1300 $cm^{-1}$ region. These features are typical for short-chain PET oligomers.

### 3.2.4 TGA analysis

The TGA curves (Figure 17) clearly show the expected decrease in thermal stability with decreasing molecular weight. PET exhibits the highest thermal stability, stable up to 400 oC before undergoing a single major degradation step.

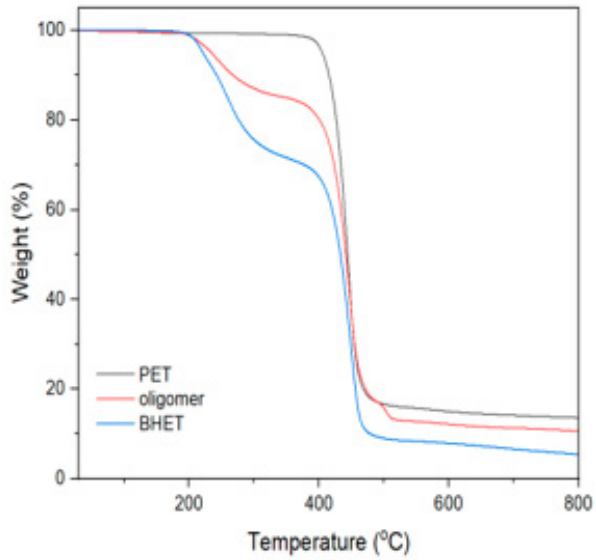


Fig. 17 Thermogravimetric analysis (TGA) curves for PET and PET glycolysis products (oligomer and BHET)

The oligomer begins to decompose earlier than PET, with the first degradation step at ca. 245oC. BHET is the least thermally stable, with degradation starting at significantly lower temperatures (ca. 220 oC) and proceeding rapidly.

### 3.2.5 Summary

The glycolysis process was successfully applied to PET bottles collected within the Circular Ocean-bound Plastic (COP) project, demonstrating the feasibility of chemical recycling for PET waste recovered from river environments. Process optimisation showed that glycolysis efficiency depends primarily on the EG/PET ratio, reaction temperature, and reaction time. The highest BHET yield (76.9%) was obtained under the optimised conditions of 197 °C, 90 min, and an EG/PET mass ratio of approx. 7.5.

The evaluated magnetic ferrite-based catalysts proved to be a promising alternative to conventional homogeneous catalysts due to their ease of separation and potential for reuse. Among the tested materials, the CFO/ZSM-5 (75/25) catalyst showed the best performance, increasing the BHET yield to 69.1% compared with 22.7% in the non-catalysed reaction. The use of magnetic catalysts simplifies post-process separation and may contribute to the development of more sustainable recycling processes.

Characterisation of the recovered products by FTIR confirmed the successful recovery of BHET with high purity. The quality of the recovered monomer was not significantly affected by PET source characteristics, including bottle colour and visible signs of environmental ageing.

**Practical implications**

Glycolysis proved to be an efficient recycling route for PET fractions recovered from riverine waste. The high BHET yields obtained for selected catalyst systems demonstrate that chemically recycled PET may serve as a valuable secondary raw material for polymer re-synthesis. However, effective implementation requires a relatively homogeneous PET stream, as any polyolefin contamination will remain unaffected under glycolysis conditions and form a residual fraction requiring further treatment or disposal. Such impurities may also complicate the separation and purification of BHET.

## 3.3 Methanolysis of PC

Polycarbonate was identified as a relevant polymer fraction within the material collected from the Aarhus River, where reusable cups and other durable consumer products were found. The presence of PC in river plastic waste highlights the need for polymer-specific recycling, as it cannot be efficiently processed with dominant polyolefins due to differences in structure, processing requirements, and properties.

Although PC can be mechanically recycled, repeated processing can cause degradation, yellowing and reduced impact strength, which may compromise its mechanical and optical properties (Singh et al., 2018). For this reason, methanolysis was investigated as an alternative route for PC, allowing cleavage of carbonate bonds and recovery of BPA.

### 3.3.1 Experimental set-up

Weighted amounts of shredded PC, catalyst (5 wt.% relative to PC, when applied), methanol as depolymerisation agent (molar ratio n(MeOH):n(PC) = 8:1), and tetrahydrofuran as co-solvent (THF; mass ratio m(THF):m(PC) = 2:1) were added into a 100 mL Teflon-lined steel autoclave or a glass flask. The mixture was heated to the target reaction temperature (60 °C or 130 °C) and maintained for the selected reaction time (3 h or longer) under autogenous pressure. After completion, the reaction mixture was filtered and the filtrate was distilled to remove unreacted methanol, THF and dimethyl carbonate (DMC). The remaining monomer fraction was recrystallised from water, followed by filtration and drying to obtain BPA (Figure 18).

Methanolysis conversion of PC and BPA yield were determined by $^{1}$H NMR analysis of the crude reaction mixtures using an internal standard (DMF). $^{1}$H NMR was also used to confirm the structural identity of the recovered BPA. FTIR spectroscopy was employed to assess the structural features and purity of the obtained monomer.


Fig. 18 Scheme of PC methanolysis and monomer recovery

### 3.3.2. Reaction efficiency

Firstly, the reaction was evaluated at 130 °C for 3 h both in the absence of a catalyst and in the presence of the following catalysts: magnesium nitrate (Mg(NO3)2), zinc acetate (Zn(OAc)2), and sodium aluminate ($NaAlO_2$). The reaction performed without a catalyst resulted in only approximately 35% conversion of PC and a BPA yield of 7%. In contrast, the use of homogeneous catalysts (magnesium nitrate and zinc acetate) or sodium aluminate led to complete PC conversion (100%) and a 95-98 % BPA yield, as determined by NMR spectroscopy (Figure 19).

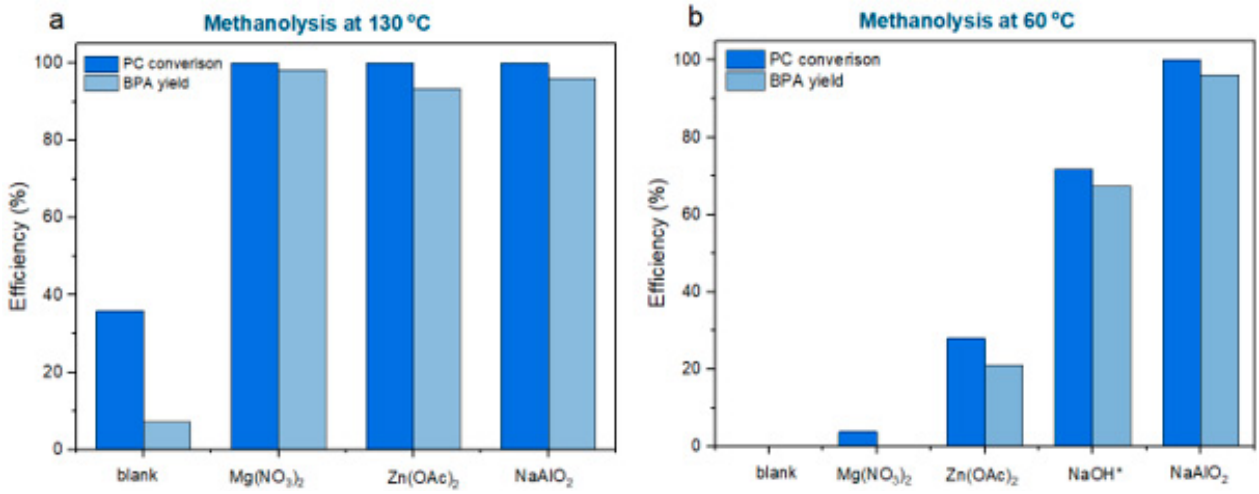


Fig. 19 Methanolysis of PC under high-temperature (130 °C) and mild (60 °C) reaction conditions. *For NaOH, 40 °C was applied

Lower reaction temperatures (60 °C) were subsequently investigated to reduce operating costs. The reaction becomes highly catalyst-dependent. Both the blank and $Mg(NO_3)_2$ conditions resulted in very low conversion, indicating insufficient activation energy at mild temperatures. $Zn(OAc)_2$ provided moderate improvement, but the highest catalytic activity was observed for NaOH (reaction carried out at 40 oC) and $NaAlO_2$, which deliver high PC conversion and BPA yields even under mild conditions.

$NaAlO_2$ was the most efficient catalyst at 60 °C, confirming its basicity and affinity for carbonate-bond activation. These results demonstrate that $NaAlO_2$ enables low-temperature depolymerisation, while other catalysts require elevated temperatures to achieve comparable performance.

Moreover, $NaAlO_2$ considered a heterogeneous catalyst, was successfully separated from the crude reaction mixture via centrifugation and reused in subsequent cycles at both 130 °C and 60 °C, similarly as reported in the literature (Krisbiantoro et al., 2024). In each case, the catalyst maintained full PC conversion and delivered a consistently high BPA yield of approx. 95%, demonstrating its high activity and potential for repeated use.

### 3.3.3. NMR analysis

The $^1$H NMR spectra of the crude reaction mixtures obtained from PC methanolysis using $NaAlO_2$ and under blank conditions confirm the formation of BPA and highlight differences in product purity depending on the catalytic system (Figure 20a). Both crude spectra contain resonances originating from residual solvents and unreacted species. Signals at approximately 3.78 ppm and 3.5 ppm correspond to dimethyl carbonate (DMC, the second monomer) and THF, while the doublet at 2.8–3.0 ppm originates from DMF (an internal standard used to calculate the reaction yield).

The crude product obtained in the presence of $NaAlO_2$ exhibits a cleaner spectral profile, with sharper BPA resonances. The characteristic aromatic multiplets (Figure 20b) between 6.6–7.2 ppm and the isopropylidene methyl singlet at approximately 1.64 ppm are significantly clearer compared with the blank reaction.

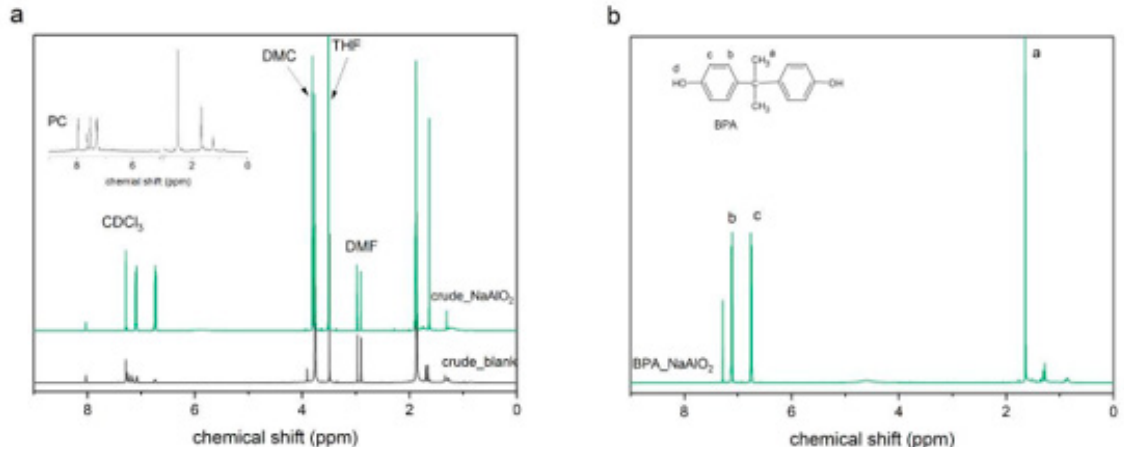


Fig. 20 $^1$H NMR spectra of: a) crude post-reaction mixtures without catalyst and with $NaAlO_2$, b) purified BPA obtained from $NaAlO_2$-catalysed methanolysis

The reference spectrum of PC included for comparison shows the typical broad and poorly resolved polymer resonances, with no discrete aromatic BPA signals in the 6.6–7.2 ppm region. The clear contrast between the PC spectrum and crude_NaALO2 spectrum confirms complete cleavage of carbonate linkages and full conversion of the polymer into its monomeric product. These features verify that the BPA is the dominant product (Jutrzenka Trzebiatowska et al., 2024).

In contrast, the blank reaction (without catalyst) shows several additional peaks at ~7.15 and ~7.22 ppm, corresponding to oligomers or BPA derivatives bearing methyl carbonate groups (as visible in PC spectrum). No DMC is formed under blank conditions; however, signals of DMC-derived species at ~3.9 ppm are visible. This behaviour is consistent with the depolymerisation mechanism: polymer swelling occurs due to solvent penetration into the PC matrix, leading to random chain scission and the formation of high-molecular-weight oligomers, followed by the formation of monomers, as reported (Kim et al., 2009). The presence of $NaAlO_2$ accelerates these processes, promoting complete cleavage of carbonate linkages and suppressing oligomer formation. Overall, the NMR results demonstrate that BPA is consistently formed across all tested conditions, while catalyst choice strongly influences the purity of the crude product.

The $^1H$ NMR spectrum of the purified BPA obtained after PC methanolysis in the presence of $NaAlO_2$ shows a clean and well-resolved set of resonances fully consistent with the literature profile of BPA (Figure 20b). The aromatic protons appear as two distinct multiplet regions between 6.6–7.2 ppm, corresponding to the ortho- and meta-protons relative to the phenolic hydroxyl groups. The isopropylidene bridge is represented by a single, sharp singlet at approximately 1.64 ppm, confirming the intact BPA core structure.

### 3.3.4 FTIR analysis

The FTIR spectra of the recovered BPA obtained using $NaAlO_2$, NaOH and $Mg(NO_3)_2$ catalysts show the characteristic vibrational features of pure BPA and confirm successful depolymerisation of polycarbonate (Figure 21). All BPA samples exhibit a broad O–H stretching band in the 3350–3500 $cm^{-1}$ region, indicating the presence of phenolic hydroxyl groups that are absent in the PC reference. Strong aromatic C=C stretching bands appear between 1600 and 1500 $cm^{-1}$, together with CH stretching vibrations at ~2960–2870 $cm^{-1}$, demonstrating preservation of the aromatic backbone. Intense C–O phenolic stretching bands at ~1220–1180 $cm^{-1}$ further confirm formation of BPA. The carbonate C=O band of polycarbonate (~1770–1790 $cm^{-1}$) is present only in the PC spectrum and completely absent in all BPA samples, indicating full cleavage of carbonate linkages.

Minor differences in band intensity among the BPA samples reflect small variations in crystallinity or

residual solvent interactions, but no signals corresponding to degradation products or incomplete depolymerisation are observed.

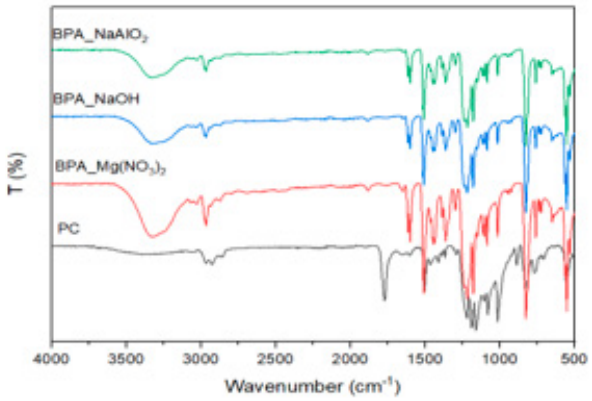


Fig. 21 FTIR spectra of BPA obtained from methanolysis of PC collected from the Aarhus River

Overall, the FTIR results verify that methanolysis efficiently converts PC into high-purity BPA regardless of the catalyst used.

### 3.3.5 Summary

Methanolysis enables complete depolymerisation of PC from river-collected OBP and recovery of high-purity BPA. $NaAlO_2$ is the most efficient catalyst, achieving full conversion at both high and mild temperatures and allowing catalyst reuse. NMR and FTIR analyses confirm the structural identity and purity of the recovered monomer.

Although PC represented a lower fraction of the collected waste, its successful depolymerisation shows that engineering plastics can also be incorporated into polymer-specific recycling strategies. Methanolysis enables selective recovery of BPA under relatively mild reaction conditions and therefore represents a promising complementary technology for dedicated PC fractions.

**Practical implications**

PC should be separated into a dedicated fraction before methanolysis, as the process is polymer-specific. The use of a co-solvent improve contact between PC and methanol and facilitate complete depolymerisation. Catalyst selection becomes important at lower temperatures, where a sufficiently active and reusable catalyst, such as $NaAlO_2$, can improve process efficiency. Future scale-up should also consider co-solvent and methanol recovery, catalyst separation and reuse, and consistent purification of the recovered BPA.

## 3.4 Pyrolysis of polyolefins (PE, PP) and PS

Pyrolysis was investigated as a chemical recycling route for selected polyolefins (PE and PP) and PS fractions collected within the Circular Ocean-bound Plastic (COP) project. Pyrolysis enables conversion of mixed polyolefin-containing waste streams into hydrocarbon fractions that can potentially be used as feedstock for the petrochemical industry.

The study focused on the influence of reaction temperature and catalyst type on polymer conversion, product distribution and product selectivity, with particular attention to the generation of liquid hydrocarbon fractions suitable for further chemical utilisation.

### 3.4.1 Experimental set-up

Pyrolysis experiments were carried out for LDPE, PP and PS in a laboratory-scale batch reactor operated under an inert nitrogen atmosphere (Figure 22). All reactions were performed at temperatures between 350 and 500 °C, with and without catalysts. A continuous nitrogen flow was maintained to ensure oxygen-free conditions and stable removal of volatile products.

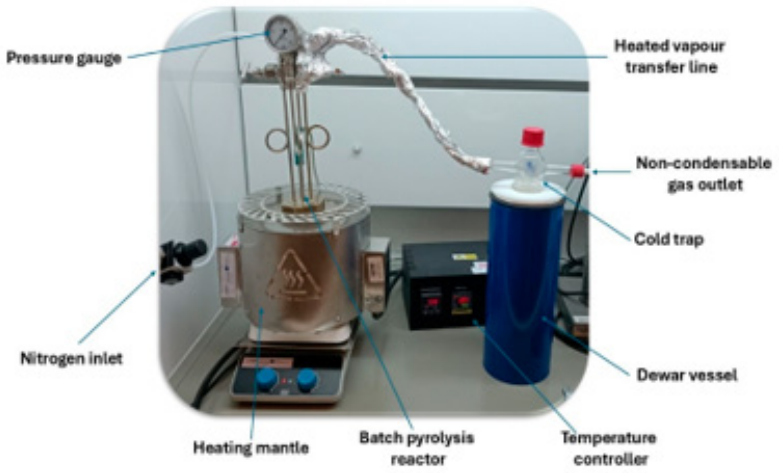


Fig. 22 Pyrolysis set-up

Weighted amounts of polymer feedstock and, when applicable, 5 wt.% catalyst (ZSM-5, SBA-15, MCM-41, CaO or ZIF-8) were introduced into the reactor. The system was then heated to the target temperature and maintained for 30 minutes. During this period, volatile pyrolysis vapours were continuously swept out of the reactor by the nitrogen stream. The vapours passed through a cooled condensation line, where liquid products (oil and wax fractions) were collected in a cold trap. Non-condensable gases were collected in gas sampling bags for subsequent GC–MS analysis, while solid residues/char remained inside the reactor.

Liquid, gaseous and solid fractions were separated and analysed individually.

- GC–MS analysis was used to determine the chemical composition of the condensed liquid and gaseous fractions obtained during pyrolysis. The technique enabled qualitative identification and semi-quantitative comparison of the main volatile and semi-volatile compounds formed during pyrolysis.
- ATR-FTIR spectroscopy and DSC analysis were applied to selected oil, wax and solid fractions to assess structural changes, functional groups and thermal behaviour.

The sample codes P1–P27 used throughout this section correspond to individual batch experiments; detailed feedstock masses, temperatures, reaction times and catalyst loadings are provided in Table S2 in the Annex C.

The physical form and colour of the recovered products varied depending on the polymer type, reaction temperature and catalyst, ranging from light polyolefin-derived oils and waxes to darker PS-derived aromatic liquids and carbonaceous solid residues (Figure 23).


Fig. 23 Representative products recovered after polymer pyrolysis: (a) gas fraction, (b) oil fraction withsome waxes/oligomers obtained from LDPE/PP, (d) oil fractions obtained from LDPE/PP, (c) wax deposits collected from the condensation system, (e) oil fraction obtained from PS, (f,h) solid residue/char, and (g) a mixture of waxes and unreacted polymer

### 3.4.2. GC-MS analysis

GC–MS analysis was performed to characterise the organic composition of the gas and oil/wax products obtained from pyrolysis of LDPE, PP and PS samples (Figure 23). The analysis was used to identify the main classes of compounds present in the pyrolysis products, including alkanes, alkenes, cyclic hydrocarbons, aromatics and others.

The results were interpreted qualitatively, as pyrolysis oils/waxes are complex mixtures containing compounds with similar fragmentation patterns and possible chromatographic overlap. It should be noted that the results are semi-quantitative. The reported percentages are based on the relative peak areas of the identified compounds in the GC–MS chromatograms and do not represent their absolute concentrations or mass yields. For PP, the class distribution of the major identified compounds was determined based on the complete GC–MS analysis to provide an overall characterisation of the product composition.

A detailed overview of the main compound classes and the ten most abundant tentatively identified compounds in each oil/wax sample is provided in Annex C, Table S3. Potential carry-over between successive experiments cannot be completely excluded because residual products may remain in the reactor, transfer lines, cold-trap system or GC–MS components.

Prior to analysis, the oil/wax samples were dissolved in hexane. GC–MS analysis was performed using a temperature programme from 40 °C to 285 °C.

#### 3.4.2.1 GC-MS analysis of gases

The gaseous products collected during pyrolysis were analysed by GC–MS to identify the main volatile compounds generated from different polymer feedstocks (LDPE, PP, PS). The results are presented in Table 5. Since nitrogen was continuously supplied to maintain an inert atmosphere during pyrolysis, it represented the dominant fraction of the collected gas samples and was excluded from the comparison of pyrolysis products. The GC–MS results therefore provide information on the relative distribution of identified volatile compounds rather than absolute gas yields (Table 5).

Table 5 Main pyrolytic gases

| Sample | Polymer | T (°C) | Catalyst | Main identified volatile compounds* |
|---|---|---|---|---|
| P4 | LDPE | 450 | None | $CO_2$ (2.6%) |
| P5 | LDPE | 450 | ZSM-5 | $CO_2$ (1.6%) |
| P12 | PP | 450 | None | 2,4-Dimethyl-1-heptene (10.0%), propene (7.4%), 2-methyl-1-pentene (5.7%), pentene (5.0%), cyclopropane (2.3%) |
| P13 | PP | 450 | ZSM-5 | Xylene (3.2%), $CO_2$ (1.5%), hexane (1.0%), propene (0.4%) |
| P16 | PP | 450 | SBA-15 | Propane (5.4%), pentene (4.9%), 2,3-dimethyl-2-butene (4.4%), 2-methylpropene (4.0%), cyclohexane (3.7%), $CO_2$ (1.3%) |
| P19 | LDPE/PP | 450 | SBA-15 | Propene (5.9%), pentane (2.8%), 2-methyl-1-pentene (1.4%), hexane (0.8%), $CO_2$ (1.6%) |
| P7 | PS | 400 | None | styrene (12.7%), toluene (2.4%), $CO_2$ (0.5%) |

| | | | | |
|---|---|---|---|---|
| P8 | PS | 400 | CaO | Benzene (9.1%), $CO_2$ (2.5%), toluene (0.5%) |
| P20 | PS | 400 | SBA-15 | CO2 (2.4%), hexane (0.2%), benzene (>0.1%), 1,3,5-Cycloheptatriene (0.2%) |
| P25 | PP | 500 | None | CO2 (2.4%), propene (0.2%); pentane (0.2%) |

*Percentages refer to the relative peak area of the identified compounds in the GC–MS chromatograms. Nitrogen was used as the carrier/purge gas during pyrolysis and therefore was not included in the comparison.

The composition of the volatile fraction was strongly dependent on the polymer type. LDPE pyrolysis at 450 °C generated only minor amounts of detectable volatile products, with $CO_2$ being the main identified compound in both non-catalytic and ZSM-5-assisted experiments.

In contrast, PP pyrolysis produced the most diverse range of volatile hydrocarbons. In the absence of a catalyst, the main identified compounds included propene, branched heptenes and pentenes, indicating extensive chain cracking and formation of light olefinic products. Catalytic pyrolysis over SBA-15 resulted in a similar hydrocarbon distribution, with propane, pentenes, branched butenes and cyclohexane identified among the main volatile products. The LDPE/PP mixture treated with SBA-15 also generated mainly light hydrocarbons, with propene being the most abundant identified compound, followed by pentane, branched pentene derivatives and hexane.

PS pyrolysis resulted mainly in aromatic hydrocarbons. For non-catalytic pyrolysis, styrene and toluene were identified, while CaO promoted benzene formation, which became the dominant detected aromatic compound.

#### 3.4.2.1 GC-MS analysis of liquid/wax of LDPE

LDPE pyrolysis was strongly temperature dependent. At 400°C, the apparent conversion was 73.7%, with 26.3 wt.% unreacted polymer and 57.1 wt.% wax, demonstrating that these conditions predominantly produced heavy products.

Therefore, higher temperatures were required to achieve extensive cracking. At 450 °C, no unreacted LDPE was recovered. ZSM-5 increased the relative oil-like contribution from 79.5% to 88.2% and decreased the wax-like contribution from 20.51% to 11.81%, while promoting a broader distribution of substituted aromatic compounds (Figure 24a). This confirms the expected catalytic cracking and aromatisation behaviour of ZSM-5.

The liquid product obtained in the presence of ZSM-5 exhibited a broad chromatographic composition (Figure 24b).

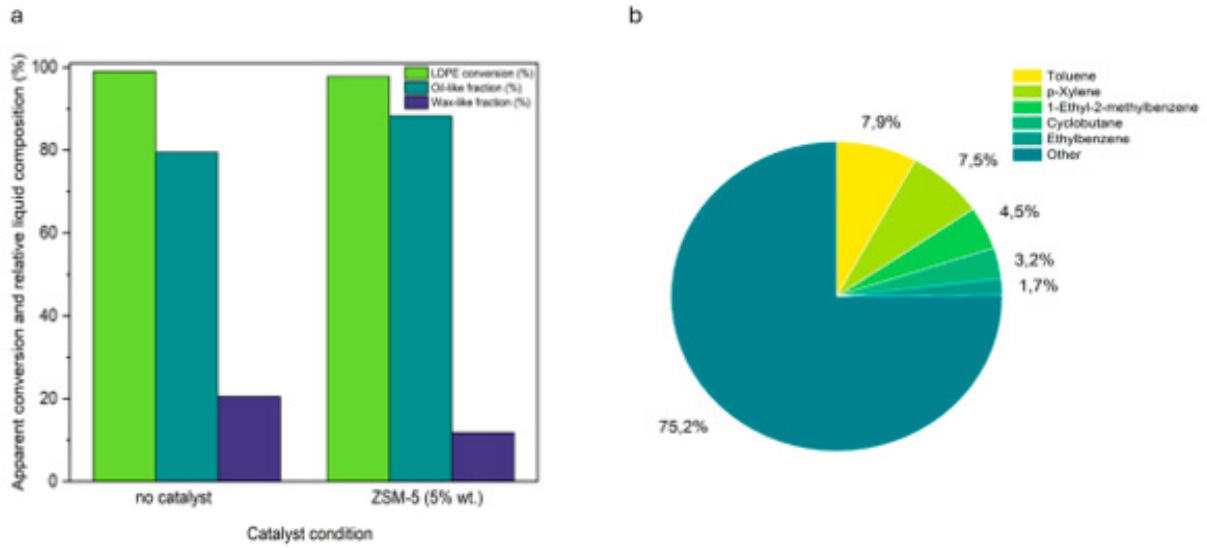


Fig. 24 a) Effect of 5 wt.% ZSM-5 on the apparent conversion of LDPE and the relative oil-like and wax-like composition of the liquid fraction obtained at 450°C for 30 min. Oil-like and wax-like contributions were operationally determined from the liquid fraction obtained from LDPE pyrolysis at 450°C for 30 min in the presence of 5 wt.% ZSM-5. Minor compounds were grouped as "Other"

### 3.4.2.2 GC-MS analysis of liquid/wax of PP

The corrected chemical-class analysis revealed distinct catalyst-dependent changes within tentatively assigned hydrocarbon fraction (Figure 25). For non-catalytic PP pyrolysis at 450 oC, acyclic olefinic, paraffinic, cyclic and aromatic hydrocarbons accounted for 55.2%, 22.8%, 14.9% and 7.2%, respectively. While the liquid fraction obtained from pyrolysis of PP at 500 °C represents a hydrocarbon-rich product dominated by branched olefins, paraffins and trace aromatics.

The major compounds include 2,4-dimethyl-1-heptene and toluene accompanied by other C7–C11 branched hydrocarbons such as nonane, 2,6-dimethyl- and octane, 3,3-dimethyl-. The fraction also contains cyclic hydrocarbons, including cyclohexane, 1,3,5-trimethyl-, as well as long-chain alkanes like hexadecane, pentacosane, heneicosane and tetracosane.

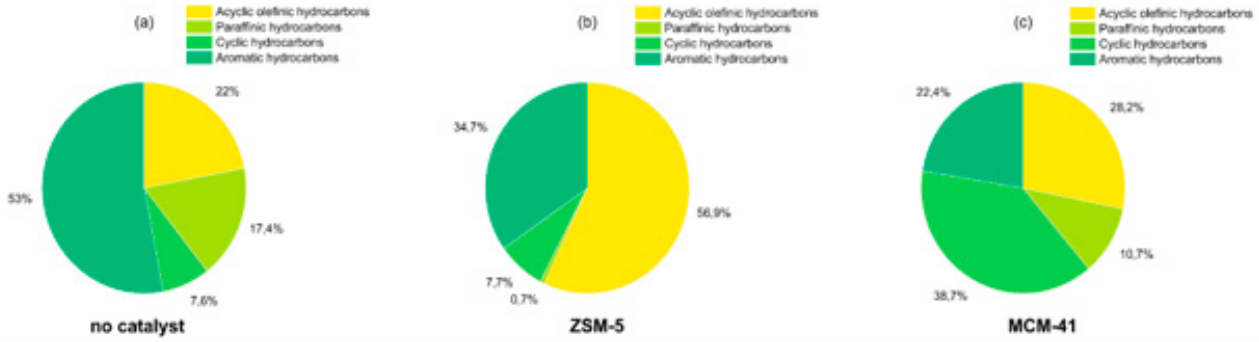


Fig. 25 Relative chemical-class distribution of the liquid products obtained from PP pyrolysis at 450°C for 30 min: (a) without a catalyst, (b) with 5 wt.% ZSM-5, and (c) with 5 wt.% MCM-41, based on GC–MS peak-area percentages

In the presence of ZSM-5, the aromatic contribution increased markedly to 52.5%, while the contributions of acyclic olefinic, paraffinic and cyclic hydrocarbons were 22.0%, 17.4% and 7.64%, respectively. This distribution is consistent with enhanced secondary cyclisation and aromatisation in the presence of ZSM-5.

For MCM-41, the assigned hydrocarbon fraction was dominated by acyclic olefinic hydrocarbons (56.9%), followed by aromatic hydrocarbons (34.7%), cyclic hydrocarbons (7.7%) and paraffinic hydrocarbons (0.7%). The very low assigned paraffinic contribution should not be interpreted as the complete absence of paraffins because only 21.8% of the total P17 chromatographic area met the adopted identification criteria. Overall, MCM-41 produced an olefin-rich but broadly distributed liquid product, whereas ZSM-5 showed the strongest selectivity towards aromatic hydrocarbons.

PP pyrolysis over SBA-15 resulted in a broad distribution of aromatic, cyclic, olefinic and paraffinic hydrocarbons. Light aromatics, including m-/p-xylene and ethylbenzene, were detected together with branched dienes, cycloalkanes and linear alkanes, indicating that SBA-15 promoted both cracking and secondary rearrangement reactions.

Because the assigned hydrocarbon fractions covered only approximately 19–25% of the complete chromatograms, the values in Figure 26 describe relative selectivity within the confidently assigned hydrocarbon fraction rather than the absolute composition or yield of the total liquid product.

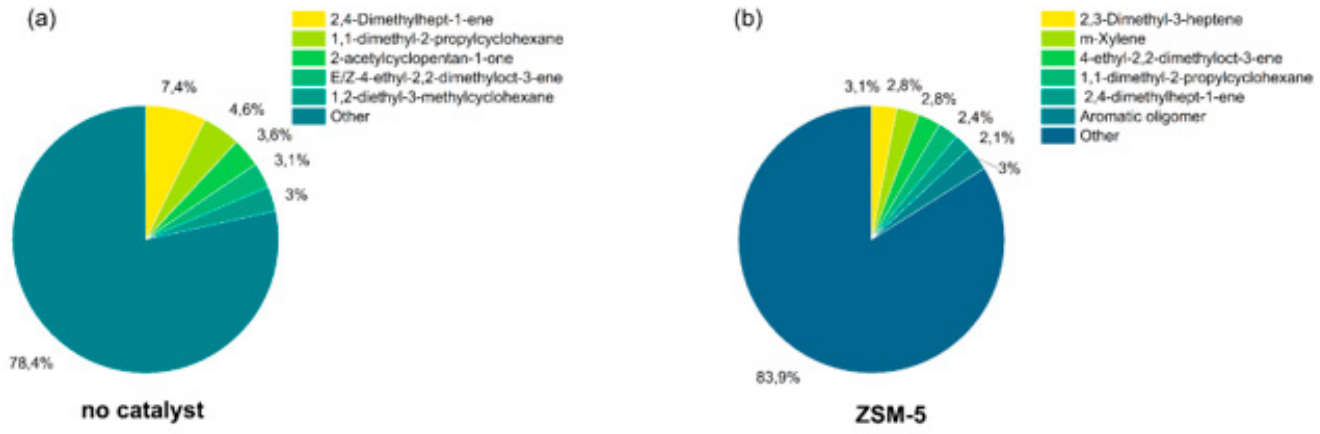


Fig. 26 Relative GC–MS peak-area distribution of the selected major compounds identified in the liquid products from PP pyrolysis at 450°C for 30 min: (a) without a catalyst and (b) in the presence of 5 wt.% ZSM-5. Minor compounds were grouped as “Other”

The compound-level distributions demonstrate that the PP-derived liquids were highly complex and were not dominated by a single molecular product. Under non-catalytic conditions, 2,4-dimethylhept-1-ene was the largest individually identified component, accounting for 7.4% of the total chromatographic peak area. In the presence of ZSM-5, the selected major compounds generally

represented approximately 2–3% or less of the complete chromatogram and included m-xylene, branched olefins and cyclic hydrocarbons. The “Other” category accounted for 78.4% and 83.9% of the P12 and P13 chromatograms, respectively, confirming broad molecular distributions and limited selectivity towards individual compounds.

Overall, catalytic pyrolysis improved the transformation of PP-derived intermediates compared with thermal pyrolysis alone. ZSM-5 showed a stronger tendency towards aromatization, whereas MCM-41 promoted broader cracking and structural rearrangement, demonstrating the role of catalyst acidity and pore structure in controlling the composition of PP pyrolysis oils.

### 3.4.2.3 GC-MS analysis of liquid of PS

GC–MS analysis showed that PS pyrolysis produced mainly aromatic compounds, with styrene-type products and aromatic oligomers as the dominant fractions. Under non-catalytic conditions, the major detected products were the $C_8H_8$ fraction (28.4%), assigned to styrene-type compounds, 1,3,5-triphenylcyclohexane (21.1%) and 2,4-diphenyl-1-butene (14.0%) (styrene dimer) (Figure 27).

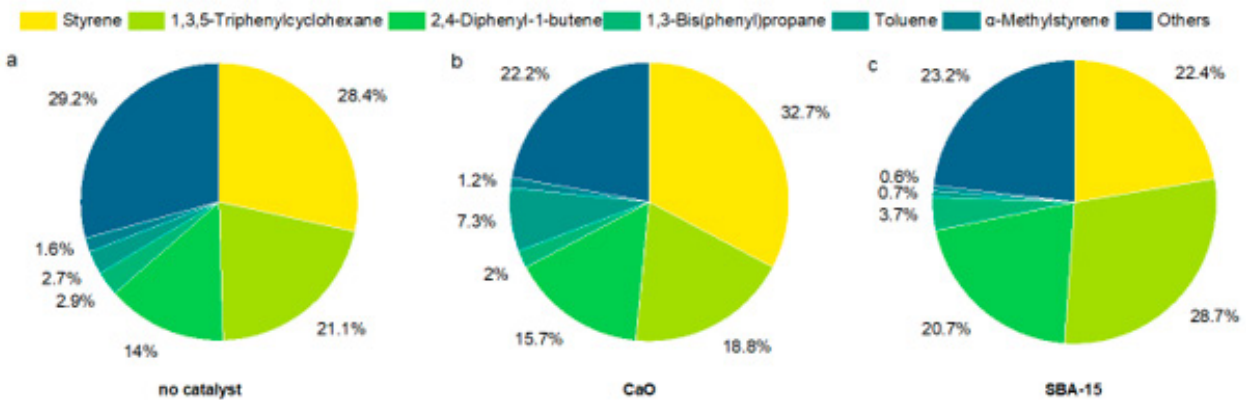


Fig. 27 Relative GC–MS peak-area distribution of the main compounds tentatively identified in the liquid products obtained from PS pyrolysis at 400°C for 30 min: (a) without a catalyst and (b) with 5 wt.% CaO, c) with 5% of SBA-15. Minor compounds were grouped as “Others”

The addition of 5 wt.% CaO increased the relative contribution of the $C_8H_8$ fraction to 32.7% and increased the formation of lighter aromatic compounds, including toluene (7.3%). At the same time, the contribution of higher molecular weight aromatic oligomers decreased, indicating a shift of the product distribution towards lower molecular weight aromatic compounds and a higher relative abundance of styrene-type products.

In contrast, ZIF-8 and SBA-15 resulted in broader product distributions, with a higher contribution of heavier aromatic structures. SBA-15 favoured the formation of oligomeric aromatic compounds, particularly 1,3,5-triphenylcyclohexane (28.7%) and 2,4-diphenyl-1-butene (20.7%), suggesting enhanced secondary condensation and oligomerization reactions. ZIF-8 showed a comparable tendency, without a noticeable increase in the relative styrene-type fraction compared with CaO.

For BaO, PS decomposition started before the reactor reached the target temperature of 400°C, suggesting a catalytic effect on the initial degradation step. Nevertheless, the product distribution was dominated by aromatic oligomers, including 1,3,5-triphenylcyclohexane (28.7%) and 2,4-diphenyl-1-butene (20.7%), with styrene accounting for 22.4%, indicating limited selectivity towards monomer recovery.

Overall, among the tested catalytic systems, CaO showed the most favourable effect on PS pyrolysis by increasing the proportion of styrene-type products and reducing the formation of heavier aromatic oligomers.

### 3.4.3 FTIR analysis of wax/oil and char

ATR-FTIR analysis supported the GC-MS results by confirming structural differences between the recovered wax and oil fractions (Figure 28).

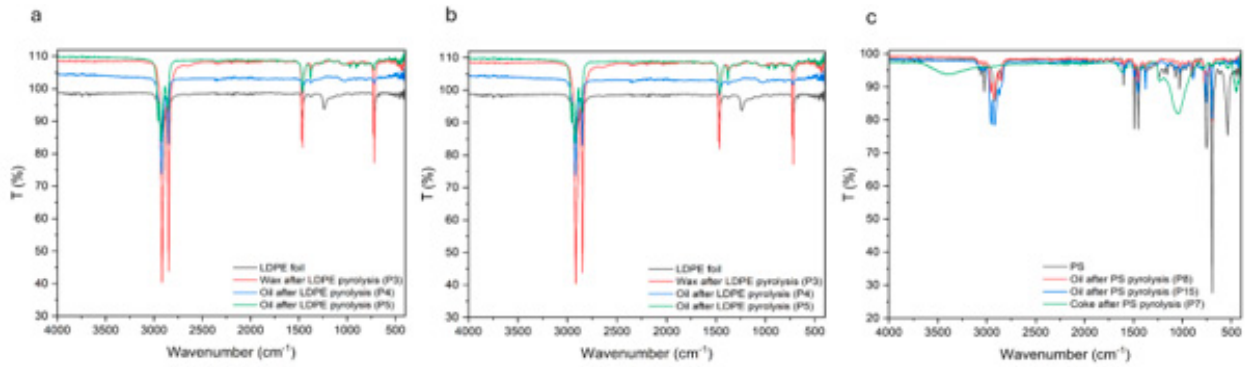


Fig. 28 Normalized ATR-FTIR spectra of pristine polymers and pyrolytic products:  and the oil and coke fractions.

The LDPE-derived wax retained the characteristic polyethylene bands (~2919 and 2850 cm $^{1}$, $CH_2$ stretching; 1463 cm $^{1}$, $CH_2$ bending; and 720 cm $^{1}$, $CH_2$ rocking), indicating the presence of relatively long polyethylene-like chains. In contrast, the oil fractions showed a higher relative intensity of the $CH_3$ band (~1377 cm $^{1}$), consistent with shorter hydrocarbon chains, while weak bands at ~1640 and 990–910 cm $^{1}$ indicated terminal vinyl groups formed during chain scission.

The PP-derived oil fractions retained the characteristic aliphatic $CH_3$ and $CH_2$ stretching bands at approximately 2950, 2918 and 2838 cm $^{1}$, together with the $CH_3$ deformation bands near 1455 and 1377 cm $^{1}$, but showed reduced intensity of the crystallinity-sensitive fingerprint bands at approximately 1000–808 cm $^{1}$. This change is consistent with the loss of the ordered isotactic PP structure and the formation of shorter, branched and predominantly non-crystalline hydrocarbons during pyrolysis. Weak absorptions near 1640 cm $^{1}$ (C=C stretching) and 990–910 cm $^{1}$ (terminal vinyl C–H out-of-plane vibrations) further support the formation of unsaturated chain-scission products. In contrast, the PP-derived wax and powder fractions retained stronger fingerprint bands characteristic

of PP, indicating the presence of higher-molecular-weight oligomers and partially converted PP-rich material.

The PS-derived oil fractions retained the characteristic aromatic C–H stretching bands in the 3080–3025 cm $^{1}$ region, aromatic ring C=C stretching bands near 1600 and 1493 cm $^{1}$, and out-of-plane aromatic C–H vibrations around 758 and 698 cm $^{1}$, confirming the preservation of phenyl groups during thermal decomposition. Additional absorptions at approximately 1630–1640 cm $^{1}$ (C=C stretching) and 990–910 cm $^{1}$ (terminal vinyl C–H out-of-plane vibrations) are consistent with the formation of vinyl-containing styrene-type products. The reduced intensity of the polymer-specific spectral pattern, together with the GC-MS results, indicates extensive chain scission and conversion of PS into aromatic monomeric and oligomeric compounds.

The solid residue obtained after PS pyrolysis showed a substantially different FTIR profile from the starting polymer, with loss of the characteristic PS bands and broad signals associated with carbonised structures.

### 3.4.4. DSC analysis of polymers and waxes

The DSC analysis was performed to evaluate the thermal behaviour, melting transitions and crystallinity of selected pyrolysis-derived waxes (P3, P22, P24) shown in Table 6.

Table 6 Thermal properties of the starting polymers and selected pyrolysis products determined by DSC

| Sample | Tm (oC) | Tc (oC) | ΔH (J/g) | Xc (%) |
|---|---|---|---|---|
| LDPE | 128.2 and 111.3 | 108.0 | 128.2 | 43.8 |
| LDPE-derived wax (P3) | 25.3 and 115.9 | 103.8 | 139.0 | 47.5 |
| PP | 167.3 | 124.5 | 83.2 | 40.2 |
| PP wax (P22) | 116.7 | 112.4 and 86.6 | 92.2 | 44.5 |
| PP wax (P24) | 36.9 and 103.3 | 76.6 and 40.6 | 118.0 | 57.0 |

DSC analysis confirmed clear differences in the thermal behaviour of the recovered polymer-derived fractions. LDPE derived wax (P3) retained characteristic PE melting transitions, although the wax exhibited an additional low-temperature melting event and slightly higher crystallinity, indicating the presence of shorter chains formed during pyrolysis.

In contrast, PP-derived waxes (P22 and P24) showed broadened and multiple melting and crystallisation

peaks, reflecting heterogeneous mixtures of PP-like domains and lower-molecular-weight pyrolysis products. These changes are consistent with extensive chain scission and structural rearrangement during thermal degradation.

### 3.4.5. XRF analysis of char

X-ray fluorescence (XRF) analysis was performed to characterise the inorganic constituents of the solid residues obtained from the pyrolysis of LDPE (P4, 450 °C) and PS (P7, 400 °C) in the absence of a catalyst. These constituents may originate from contamination, pigments or fillers present in the feedstock.

The XRF analyses were performed according to standard PN-EN 15309:2010. XRF results are normalised to 100%, therefore, the reported values represent the relative proportions of the detected elements and should not be interpreted as absolute concentrations in the char.

Table 7 Summary of dominant inorganic elements in char samples determined by XRF

| Sample | Elemental composition of LDPE pyrolysis char determined by XRF (normalised to 100%), % (m/m) |
|---|---|
| LDPE (P4) | Si 38.3%, Ca 15.7%, Fe 13.8%, K 7.5%, Al 6.8%, Mn 5.6%, Cl 4.3%, S 2.7%, P 2.13%, Mg 1.2% and Ti, Zn, Cr |
| PS (P7) | Si 40.1%, Ca 25.3%, Br 12.2%, Fe 7.1%, K 3.8%, Al 2.6%, S 1.8%, Cl 1.5%, P 1.4%, Mg 1.3% and Zn, Mn, Ti, Na, Cr, Cu |

The LDPE pyrolysis char was characterised by a predominance of Si, which accounted for 38.3% of the normalised elemental composition, followed by Ca (15.7%) and Fe (13.8%). Other relatively abundant elements included K (7.5%), Al (6.8%), Mn (5.6%), and Cl (4.2%), while S (2.7%), P (2.13%), Mg (1.2%) were detected at lower relative proportions. Ti, Zn and Cr were also detected, but at comparatively low levels.

A similar predominance of Si was observed for the PS pyrolysis char, where it accounted for 40.1% of the normalised elemental composition. Ca was the second most abundant element (25.3%), followed by Br (12.2%) and Fe (7.1%). The relatively high proportion of Br may indicate the presence of brominated flame-retardant additives, which are commonly used in expanded polystyrene. The remaining major detected elements included K (3.9%), Al (2.6%), S (1.8%), Cl (1.5%), P (1.4%), Mg (1.3%), while Zn, Mn, Ti, Na, Cr and Cu were present at lower relative proportions.

Overall, both pyrolysis chars exhibited a similar predominance of Si and Ca, although differences were observed in the relative distribution of the other detected elements. The PS char was characterised by a notably higher relative proportion of Ca and the presence of a substantial Br contribution.

These differences may reflect variations in the inorganic additives, fillers, pigments, or other mineral components originally present in the polymer materials and concentrated in the solid residue during pyrolysis.

### 3.4.6 Analysis of fresh and spent catalyst

ATR-FTIR spectra (Figure 29a) of fresh and spent ZSM-5, SBA-15 and MCM-41 retained the principal silicate-framework absorptions after PP pyrolysis, indicating that no major framework degradation was detectable under the applied conditions. Additional or enhanced aliphatic absorptions in the spent materials were consistent with hydrocarbons retained on the catalyst surface.

TGA analysis further supported these observations (Figure 29b). All spent catalysts showed higher mass losses compared with their corresponding fresh materials, reflecting the presence of retained hydrocarbons and carbonaceous deposits formed during pyrolysis.

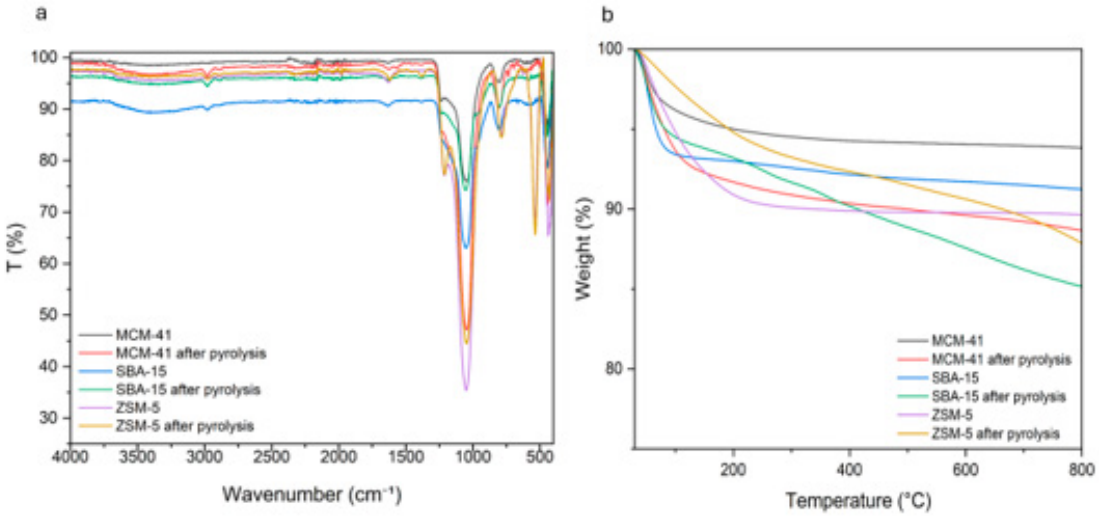


Fig. 29 FTIR-ATR (a) and TGA (b) of the fresh and spent (after pyrolysis) catalysts

FTIR and TGA therefore indicate that the catalyst structures were largely retained after PP pyrolysis, while additional hydrocarbon/carbonaceous deposits were present on the spent catalysts.

### 3.4.7 Summary

Pyrolysis was evaluated as a chemical recycling route for LDPE, PP and PS fractions collected within the Circular Ocean-bound Plastic (COP) project. The results demonstrate that pyrolysis can convert selected polyolefins and PS into hydrocarbon-rich products, while the product distribution is strongly dependent on polymer type, reaction temperature and catalyst selection. Polyolefin pyrolysis produced mainly aliphatic, cyclic and aromatic hydrocarbons, whereas PS pyrolysis generated predominantly aromatic monomeric and oligomeric products.

For LDPE, increasing the reaction temperature from 400 to 450 oC promoted complete polymer conversion and reduced wax formation, while ZSM-5 enhanced secondary cracking and aromatisation, increasing the relative proportion of oil-like products. PP pyrolysis yielded complex hydrocarbon mixtures of branched olefins, paraffins, cyclic hydrocarbons and aromatics. ZSM-5 strongly increased the aromatic contribution, MCM-41 resulted in a more olefin-rich product distribution, whereas SBA-15 produced a broadly distributed hydrocarbon fraction. PS pyrolysis produced mainly aromatic compounds, including styrene-type products and aromatic oligomers. Among the tested catalysts, CaO gave the most favourable product distribution, increasing the relative contribution of styrene-type products while reducing heavier aromatic oligomers.

FTIR and DSC analyses supported the structural changes observed after pyrolysis, while XRF showed that inorganic components (Si, Ca and Fe among the dominant elements) present in the collected plastics were concentrated in the solid residues.

The results demonstrate that pyrolysis is a promising complementary recycling route for contaminated or degraded OBP fractions that are unsuitable for mechanical recycling. Appropriate catalyst selection enables tailoring of the product composition, with ZSM-5 promoting aromatisation of polyolefins and CaO improving the recovery of styrene-type products from PS.

**Practical implications**

Pyrolysis can be applied to selected PE, PP and PS fractions, but the resulting product composition depends strongly on feedstock type and operating conditions. Catalyst selection provides some control over product distribution, as demonstrated by the increased aromatic contribution obtained with ZSM-5 for polyolefins and the higher relative contribution of styrene-type products obtained with CaO for PS. Further work should focus on complete mass balances, quantitative product yields, catalyst stability and product upgrading before pilot-scale implementation.

## 3.5. Up-scale pyrolysis trials performed by Plast Center Danmark

To evaluate the applicability of chemical recycling under semi-industrial conditions, up-scale batch pyrolysis trials of selected PP and PE fractions collected from Aarhus River were performed by the Plast Center Danmark (PCD) in cooperation with Waste2Value. These results are described in detail in a separate report “Up-scale Pyrolysis of Selected Aarhus River Plastic” by G. Mihut and H. Tüzün.

The study compared contaminated, washed and virgin PP and PE blend (approx. 60% LDPE and 40% HDPE) under an inert nitrogen atmosphere. Prior to processing, the materials were manually sorted and mechanically ground. The trials generated three primary product fractions: condensable oil/wax,

non-condensable gas, and solid char. The oil/wax and char fractions were collected and quantified, while the non-condensable gas fraction was not collected and was therefore estimated from the overall mass balance. Product characterisation included density measurements, determination of the total acid number (TAN), FTIR analysis, GC–MS analysis, XRF analysis, ICP analysis and TGA. These analyses were used to evaluate the physicochemical properties and composition of the obtained pyrolysis products. The pyrolysis results are summarised in Table 8.

Table 8 Results of pilot-scale pyrolysis of PP and PE fractions

| Material, condition | Oil/wax yield (%) | Char yield (%) | Gas fraction (%) | Density (g/mL) | TAN (mg KOH/g) | Main analytical findings |
|---|---|---|---|---|---|---|
| Aarhus River PP, untreated | 79.5 | 0.4 | 20.1 | 0.79 | 4.2 | PP-derived aliphatic and unsaturated hydrocarbons; highest measured acidity; inorganic contamination retained mainly in char |
| Aarhus River PP, untreated (repeat) | 78.9 | 1.0 | 20.1 | 0.80 | 1.3 | Similar results in yield to the first trial; PP-derived branched, cyclic and unsaturated hydrocarbons; |
| Reference PP, virgin | 66.4 | 0.2 | 33.4 | 0.76 | 0.5 | Similar principal hydrocarbon structure to river PP oils; lower acidity than contaminated PP |
| Aarhus River PP, washed | 73.1 | 0.1 | 26.8 | 0.81 | 0.4 | Washing did not substantially change the main oil/wax hydrocarbon profile, but reduced acidity compared with contaminated PP |
| Aarhus River PE blend, untreated | 37.6 | 1.5 | 60.9 | 0.71 | 0.4 | Mainly linear long-chain alkanes and alkenes; substantially lower condensable yield and higher calculated gas/loss fraction than virgin PE |
| Reference blend PE, virgin | 86.2 | 0.2 | 13.6 | 0.81 | 0.2 | Mainly linear C10 to >C26 alkanes and alkenes; highest oil/wax yield and lowest gas/loss fraction |

River-collected PP produced repeatable oil/wax yields of approximately 79%, while the washed and virgin samples gave 73.1% and 66.4%, respectively; char formation remained low at 0.1–1.0%. The condensable products were dominated by PP-derived aliphatic, branched, cyclic and unsaturated hydrocarbons, whereas inorganic contaminants were mainly retained in the solid residue. Washing reduced the acidity of the resulting products without substantially altering their hydrocarbon composition.

The contaminated PE fraction exhibited a substantially lower condensable yield (approximately 38 wt.%) and a considerably higher gas fraction than the corresponding virgin material, highlighting the importance of feedstock composition, contamination level, and process conditions. The PE-derived

products were composed mainly of linear alkanes and alkenes ranging from approximately C10 to C26 and higher.

XRF and ICP analyses of char identified the presence of calcium, silicon, iron, aluminium, chlorine, titanium, copper, and lead compounds originating from fillers, pigments, and environmental contamination.

Overall, the up-scale trials demonstrated that pyrolysis represents a promising complementary recycling route for polyolefin-rich ocean-bound plastic streams that are unsuitable for conventional mechanical recycling. However, the results also underline the importance of feedstock sorting, cleaning, and process optimisation to achieve stable product quality and maximize resource recovery.

Full process conditions, mass balances and FTIR, GC-MS, XRF, ICP and TGA results are provided in the dedicated partner report. For detailed trial procedures and analytical results, see the separate report "Up-scale Pyrolysis of Selected Aarhus River Plastic".

## 3.6 Comparison of laboratory- and up-scale pyrolysis experiments

The laboratory-scale experiments performed at the University of Gdańsk (UG) and the up-scale trials carried out by Plast Center Danmark (PCD) focused on different aspects of the pyrolysis process. While the UG experiments focused on the optimisation of process parameters and the identification of reaction pathways under controlled laboratory conditions, the PCD trials evaluated the technical feasibility of pyrolysis under conditions closer to industrial implementation.

The laboratory-scale experiments performed at UG investigated the influence of temperature and catalyst type (ZSM-5, SBA-15, MCM-41, CaO and ZIF-8) on the conversion of LDPE, PP and PS fractions. Emphasis was placed on product selectivity and the chemical composition of the resulting oils, waxes and gaseous products. The up-scale trials carried out by PCD focused primarily on mixed and contaminated polyolefin streams recovered from the Aarhus River. Rather than maximising the yield of individual compounds, these experiments evaluated the influence of feedstock heterogeneity and contamination on overall process performance, product yield and product quality.

For PP-derived oil/wax fractions, FTIR and GC–MS analyses of the up-scale pyrolysis products showed consistent results, with the oil/wax fraction consisting mainly of branched, cyclic, and unsaturated hydrocarbons. A similar product composition was observed in the non-catalytic laboratory-scale experiments. For PE-derived oil/wax fractions, FTIR and GC–MS analyses of the both laboratory- and up-scale pyrolysis products showed that the oil/wax fraction consisted of long-chain aliphatic

hydrocarbons. These findings demonstrate good comparability between the two scales, indicating that the principal product chemistry of non-catalytic PP or PE pyrolysis was maintained during up-scaling.

Another common observation was the retention of inorganic constituents in the solid residue. XRF analyses from both studies showed that elements such as Si, Ca, Fe, and Al were predominantly concentrated in the char. Although the specific elemental composition varied depending on the feedstock, the findings consistently demonstrated that inorganic contaminants and mineral matter are retained in the solid residue rather than transferred to the condensable hydrocarbon fraction.

Despite differences in reactor design, scale and feedstock composition, both studies revealed several common trends:

- PP exhibited higher conversion efficiency than PE.
- Product composition was strongly dependent on the initial polymer structure, with PP producing branched hydrocarbons and PE yielding predominantly linear compounds.
- Both studies demonstrated that impurities and inorganic contaminants remain concentrated mainly in the solid residue rather than in the liquid fraction.

Taken together, the two experimental approaches provide complementary information that supports the implementation of pyrolysis as a viable recycling route for selected OBP. The laboratory-scale experiments supplied detailed mechanistic insights and enabled catalyst evaluation, whereas the up-scale trials demonstrated the practical applicability of the process to real and heterogeneous waste streams.

# 4.
# Conclusion

# 4. Conclusion

This report evaluated solvent-based and chemical recycling pathways for heterogeneous OBP fractions collected from the Motława River (Poland) and the Aarhus River (Denmark) as part of the Interreg South Baltic Circular Ocean-bound Plastic (COP) project. River-collected materials can be considered a technically relevant secondary raw material, but their recycling potential depends on polymer type, contamination level and environmental degradation.

The heterogeneous nature of OBP prevents the application of a single recycling technology for all polymer types and instead requires differentiated, polymer-specific processing strategies tailored to the characteristics and condition of each fraction. Efficient valorisation requires a cascade approach combining sorting, cleaning, material identification and selection of the recycling route according to polymer type and material condition. Mechanical recycling should remain the preferred option for clean, rigid and homogeneous fractions, while chemical recycling should be applied where mechanical processing cannot ensure sufficient material quality.

Solvent-based recycling is a promising route for PP and PE fractions. Dissolution–precipitation enabled recovery of purified polymer material while largely preserving their characteristic chemical and thermal properties. This approach is particularly relevant where the polymer itself remains valuable and does not require depolymerisation. Among the investigated solvents, p-cymene provided favourable results. However, the observed changes in PP oxidation and crystallinity show that temperature control and stabilisation may be required to maintain material quality.

Chemical depolymerisation was a suitable recycling route for condensation polymers present in OBP. PET glycolysis enabled the recovery of the monomer, BHET, with an optimised yield of approximately 76.9%, showing that environmentally exposed PET with reduced suitability for direct mechanical recycling can still serve as a feedstock for chemical recycling. Similarly, PC methanolysis provided an effective polymer-specific route for recovering its monomer - BPA. The use of heterogeneous catalysts in these processes offers an additional advantage by facilitating catalyst separation, recovery and reuse in subsequent reaction cycles.

Pyrolysis provided a feasible route for selected LDPE, PP and PS fractions. The laboratory experiments demonstrated that temperature and catalyst selection strongly affect product distribution, with ZSM-5 promoting aromatisation of polyolefin-derived products, MCM-41 favouring olefin-rich products, and CaO increasing the relative contribution of styrene-type products from PS. The up-scale trials confirmed that river-collected PP can generate repeatable condensable oil/wax fractions with low char

formation, while the substantially lower condensable yield obtained from untreated river-collected PE highlights the importance of feedstock quality and contamination control. XRF analysis shows that pyrolysis chars contain notable levels of inorganic elements, mainly Si, Ca and Fe, confirming that mineral fillers, pigments and environmental contaminants present in OBP accumulate in the solid residue during the process.

# 5.
# Recommendations

# 5. Recommendations

Based on the results obtained within the Circular Ocean-bound Plastic project, the following recommendations are proposed for future development of OBP recycling pathways:

- Prioritise polymer identification and sorting. Recycling efficiency strongly depends on polymer type and material purity. Collected OBP should be separated into stable and sufficiently homogeneous fractions, with particular attention to PP, PE, PET, PS and PC streams.
- Standardise cleaning procedures. Removal of organic residues, dirt and moisture should be treated as an essential pre treatment step to ensure stable processing and predictable product quality. Link to Report: "Pathways for Cleaning Collected Ocean-Bound Plastic" https://circularoceanplastic.eu/report-pathways-for-cleaning-collected-ocean-bound-plastic/
- Apply the least intensive suitable recycling route first. Clean and homogeneous fractions should preferably be directed towards mechanical recycling. Solvent-based purification should be considered when the polymer remains structurally valuable but requires removal of contaminants or additives. Depolymerisation should be applied to suitable condensation or engineering polymers, while pyrolysis should be reserved for selected fractions that cannot be effectively managed through less intensive routes.
- Use solvent-based recycling for relatively clean PE and PP fractions. This route is appropriate where polymer recovery is preferable to depolymerisation. Future development should prioritise solvent recovery and reuse, as solvent consumption significantly affects environmental performance and process economics.
- Use depolymerisation technologies selectively, including glycolysis or methanolysis for condensation polymers such as PET, PC, PA to maximise recovery of monomers.
- Prioritise heterogeneous catalysts where possible. Heterogeneous catalysts allow easier separation from the reaction mixture and offer the possibility of catalyst recovery and reuse. Further work should focus on improving their activity, stability and recyclability under real OBP conditions.
- Consider pyrolysis for selected degraded or difficult-to-recycle polyolefin- and PS-rich fractions. Pyrolysis should be considered where mechanical recycling or selective solvent-based/depolymerisation routes are technically unsuitable, provided that the feedstock is sufficiently characterised and prepared to ensure stable process operation and predictable product quality.
- Optimise catalyst selection according to the desired products, as catalyst chemistry strongly affects hydrocarbon composition and product selectivity.
- Integrate chemical recycling with existing mechanical recycling systems to maximise overall material recovery and minimise disposal of river-collected plastics.
- Future work should include life-cycle assessment (LCA), techno-economic analysis (TEA), catalyst

optimisation, solvent recovery, and scale-up studies under continuous processing conditions.

# 6. Limitations of the study

# 6. Limitations of the study

This study was conducted at laboratory scale using representative polymer fractions recovered within the COP project. Although the investigated materials reflect the main polymer streams identified in the project, they do not capture the full variability and heterogeneity of river-collected plastic waste. Product yields, particularly for pyrolysis experiments, were assessed primarily through analytical characterisation rather than complete mass balance calculations. In addition, the GC–MS analyses provided semi-quantitative information on product composition and distribution.

The primary objective of this work was to evaluate the technical feasibility of selected recycling routes. Consequently, process optimisation focused on laboratory-scale performance rather than comprehensive techno-economic or environmental assessment. Key aspects required for industrial implementation including continuous reactor operation, process scale-up, solvent recovery, catalyst lifetime and regeneration, process integration, as well as life-cycle assessment (LCA) and techno-economic analysis were beyond the scope of this deliverable.

Therefore, the proposed recycling pathways should be regarded as technically promising laboratory- and partner-scale solutions that require further optimisation and pilot-scale verification before industrial deployment.

# 7.
# References

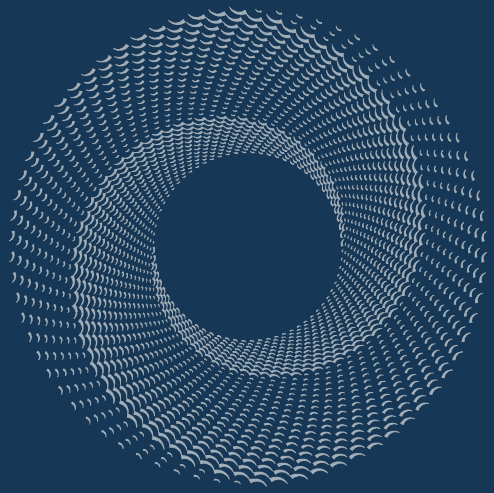

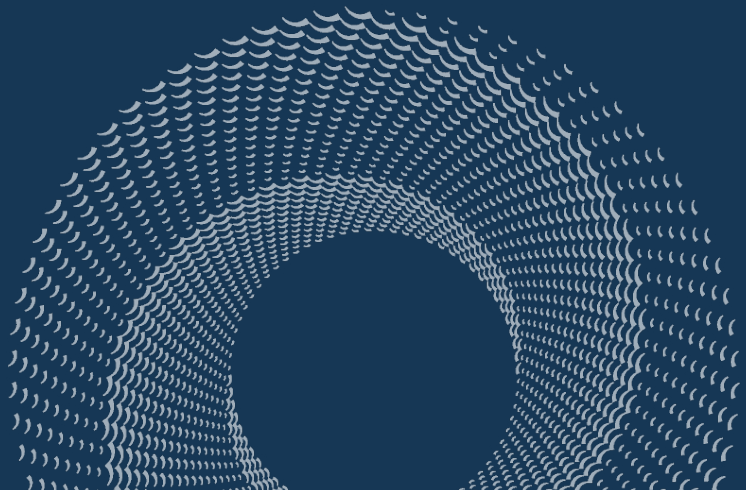

# 7. References


Datta, J., & Kopczyńska, P. (2016). From polymer waste to potential main industrial products: Actual state of recycling and recovering. Critical Reviews in Environmental Science and Technology, 46(10), 905–946. https://doi.org/10.1080/10643389.2016.1180227

European Environment Agency. (2024, May 23). Plastics recycling in Europe: obstacles and options. https://www.eea.europa.eu/en/european-zero-pollution-dashboards/indicators/plastics-recycling-in-europe-obstacles-and-options

Ganzer, S., Narra, M.-M., Mensah, I., & Narra, S. (2024). Plastic waste streams into the South Baltic Sea – On a country level. https://circularoceanplastic.eu/wp-content/uploads/2024/12/Plastic-waste-streams-into-the-South-Baltic-Sea-On-a-country-level_2024.pdf

Gontarek-Castro, E., Gołąbiewska, A., & Jutrzenka Trzebiatowska, P. (2025). Pathways for cleaning collected ocean-bound plastic. https://circularoceanplastic.eu/wp-content/uploads/2025/02/Rapport_Pathways-for-cleaning-collected-Ocean-bound-Plastic_2025.pdf

Gontarek-Castro, E., Haseler, M., Narra, M. M., Gołąbiewska, A., & Jutrzenka Trzebiatowska, P. (2026). Utilization routes of plastic waste from the marine environment: a review. In Waste Management (Vol. 210). Elsevier Ltd. https://doi.org/10.1016/j.wasman.2025.115221

González-Fernández, D., Hanke, G., Pogojeva, M., Machitadze, N., Kotelnikova, Y., Tretiak, I., Savenko, O., Bilashvili, K., Gelashvili, N., Fedorov, A., Kulagin, D., Terentiev, A., & Slobodnik, J. (2022). Floating marine macro litter in the Black Sea: Toward baselines for large scale assessment. Environmental Pollution (Barking, Essex: 1987), 309(119816), 119816. https://doi.org/10.1016/j.envpol.2022.119816

Harasymchuk, I., Kočí, V., & Vitvarová, M. (2024). Chemical recycling: comprehensive overview of methods and technologies. International Journal of Sustainable Engineering, 17(1), 124–148. https://doi.org/10.1080/19397038.2024.2409162

Hou, Q., Zhen, M., Qian, H., Nie, Y., Bai, X., Xia, T., Laiq Ur Rehman, M., Li, Q., & Ju, M. (2021). Upcycling and catalytic degradation of plastic wastes. In Cell Reports Physical Science (Vol. 2, Number 8). Cell Press. https://doi.org/10.1016/j.xcrp.2021.100514

Ibrahim, I. A., Khoo, K. S., Rawindran, H., Lim, J. W., Ng, H. S., Shahid, M. K., Tong, W. Y., Hatshan, M. R., Sun, Y. M., Lan, J. C. W., Chan, Y. J., & Usman, A. (2023). Environmental Sustainability of Solvent Extraction Method in Recycling Marine Plastic Waste. Sustainability (Switzerland), 15(22), 15742. https://doi.org/10.3390/su152215742

Jutrzenka Trzebiatowska, P., Maramorosz, Z., Baluk, M. A., Gazda, M., Eceiza, A., & Zaleska-Medynska, A. (2024). The catalytic activity of metal–organic frameworks (MOFs) and post-synthetic modified MOF towards depolymerisation of polycarbonate. Applied Surface Science, 673. https://doi.org/10.1016/j.apsusc.2024.160894

Kim, D., Kim, B. K., Cho, Y., Han, M., & Kim, B. S. (2009). Kinetics of polycarbonate methanolysis by a consecutive reaction model. Industrial and Engineering Chemistry Research, 48(14), 6591–6599. https://doi.org/10.1021/ie801893v

Kosloski-Oh, S. C., Wood, Z. A., Manjarrez, Y., De Los Rios, J. P., & Fieser, M. E. (2021). Catalytic methods for chemical recycling or upcycling of commercial polymers. In Materials Horizons (Vol. 8, Number 4, pp. 1084–1129). Royal Society of Chemistry. https://doi.org/10.1039/d0mh01286f

Krisbiantoro, P. A., Sato, M., Lin, T. M., Chang, Y. C., Peng, T. Y., Wu, Y. C., Liao, W., Kamiya, Y., Otomo, R., & Wu, K. C. W. (2024). Low-Temperature Methanolysis of Polycarbonate over Solid Base Sodium Aluminate. Langmuir, 40(10), 5338–5347. https://doi.org/10.1021/acs.langmuir.3c03799

Lebreton, L., van der Zwet, J., Damsteeg, J.-W., Slat, B., Andrady, A., & Reisser, J. (2017). River plastic emissions to the world's oceans. Nature Communications, 8(1). https://doi.org/10.1038/ncomms15611

Manzoor, S., Naqash, N., Rashid, G., & Singh, R. (2022). Plastic Material Degradation and Formation of Microplastic in the Environment: A Review. Materials Today: Proceedings, 56, 3254–3260. https://doi.org/10.1016/j.matpr.2021.09.379

Mark, L. O., Cendejas, M. C., & Hermans, I. (2020). The Use of Heterogeneous Catalysis in the Chemical Valorization of Plastic Waste. In ChemSusChem (Vol. 13, Number 22, pp. 5808–5836). Wiley-VCH Verlag. https://doi.org/10.1002/cssc.202001905

Mihut, G. (2026). Mechanical tests & material analysis on recycled samples. https://circularoceanplastic.eu/wp-content/uploads/2026/03/2026-03-Mechanical-tests-and-material-analysis-PCD.pdf

Mihut, G., Tüzün, H., Jutrzenka Trzebiatowska, P., & Gontarek-Castro, E. (2026). Polymer composition of river-collected plastic. https://circularoceanplastic.eu/wp-content/uploads/2026/05/Polymer-composition-of-river-

collected-plastic.pdf

Plastics Europe. (n.d.). CHEMICAL RECYCLING AND THE ROLE OF MASS BALANCE EXPLAINED.

Ragaert, K., Delva, L., & Van Geem, K. (2017). Mechanical and chemical recycling of solid plastic waste. In Waste Management (Vol. 69, pp. 24–58). Elsevier Ltd. https://doi.org/10.1016/j.wasman.2017.07.044

Singh, R., Shahi, S., & Geetanjali. (2018). Chemical Degradation of Poly(bisphenol A carbonate) Waste Materials: A Review. In ChemistrySelect (Vol. 3, Number 42, pp. 11957–11962). Wiley-Blackwell. https://doi.org/10.1002/slct.201802577

Tarani, E., Arvanitidis, I., Christofilos, D., Bikiaris, D. N., Chrissafis, K., & Vourlias, G. (2023). Calculation of the degree of crystallinity of HDPE/GNPs nanocomposites by using various experimental techniques: a comparative study. Journal of Materials Science, 58(4), 1621–1639. https://doi.org/10.1007/s10853-022-08125-4

Yun, L. X., Wei, Y., Sun, Q., Li, Y. T., Zhang, B., Zhang, H. T., Shen, Z. G., & Wang, J. X. (2023). Magnetic hollow micro-sized nanoaggregates for synergistically accelerating PET glycolysis. Green Chemistry, 25(17), 6901–6913. https://doi.org/10.1039/d3gc01762a

Zhang, C.-Y., & Nakatani, J. (2024). Implications of chemical recycling of plastic waste for climate change impacts: A critical review. Sustainable Production and Consumption, 48, 301–323. https://doi.org/10.1016/j.spc.2024.05.016

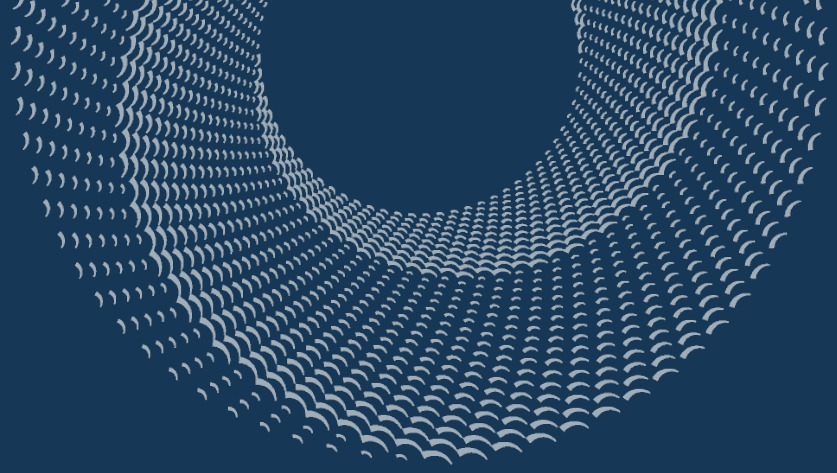

# Circular Ocean-bound Platic

Breaking the waves of ocean plastic pollution
- From source to solution

**www.circularoceanplastic.eu**

The report is co-funded by:

COP Circular Ocean-Bound Plastic | Interreg South Baltic | Co-funded by the European Union | Operation of Strategic Importance